https://doi.org/10.5194/egusphere-2022-1475
Preprint. Discussion started: 9 January 2023

Structural framework and timing of the Pahtohavare Cu ± Au deposits, Kiruna mining district, Sweden

Leslie Logan[1], Ervin Veress[1], Joel B.H. Andersson[1], Olof Martinsson[1], Tobias E. Bauer[1]

[1]Division of Geosciences and Environmental Engineering, Luleå University of Technology, Luleå SE-971 87, Sweden

Correspondence to: Leslie Logan (Leslie.logan@ltu.se)

Abstract. As part of a larger mineral systems approach to Cu-bearing mineralization in northern Norrbotten, this study utilizes structural geology to set the classic Pahtohavare Cu ± Au deposits into an up-to-date tectonic framework. The Pahtohavare Cu ± Au deposits, situated only 5 km SW of the Kiirunavaara world-class iron oxide apatite (IOA) deposit, have a dubious timing and their link to IOA formation is not constrained. The study area contains both epigenic Cu ± Au (Pahtohavare) and iron oxide-copper-gold (IOCG, Rakkurijärvi) mineral occurrences which are hosted in bedrock that has been folded and bound by two shear zones trending NE-SW and NW-SE to the east and southwest, respectively. Structural mapping and petrographic investigation of the area reveal an anticlinal, noncylindrical, SE-plunging fold geometry. The cleavage measurements mirror the fold geometry which characterizes the fold as F_2 associated to the late phase of the Svecokarelian orogeny. Porphyroclasts with pressure shadows and mylonitic fabrics observed in thin section indicate S_0/S_1 is a tectonic fabric. The epigenetic Pahtohavare Cu ± Au mineralization sit in brittle-ductile structures that cross cut an earlier foliation and the F_2 fold, indicating that the timing of the deposits occurred syn- to post-F_2 folding, at least ca. 80 Myr after the Kiirunavaara IOA formation. A 3D model and cross sections of the Pahtohavare-Rakkurijärvi area and a new structural framework of the district are presented and used to suggest that the shear zones bounding the area are likely reactivated early structures that have played a critical role in ore formation in the Kiruna mining district.

1 Introduction

The Kiruna mining district is situated in the northern Norrbotten ore province (Martinsson et al., 2016) which has abundant Fe and Cu-Au mineralization, extensive Na-Ca metasomatism (Frietsch et al., 1997), and regional crustal-scale fault structures (Bergman et al., 2001). Multiple styles of mineralization are hosted in Rhyacian to Orosirian rocks with major ore forming periods related to the Orosirian Svecokarelian orogeny (ca. 1.9 to 1.8 Ga; Bergman et al., 2001; Martinsson et al., 2016). The orogeny was polyphase and resulted in complex overprinting alteration assemblages, metamorphic events, structures, and mineralization regionally (e.g. Wright, 1988; Bergman et al., 2001; Wanhainen et al., 2012; Martinsson et al., 2016; Bergman, 2018; Andersson et al., 2021; Bauer et al., 2022). Radiometric studies point to abundant iron oxide apatite (IOA) and Cu-Au mineralization processes during the early orogenic phase of the Svecokarelian orogeny (ca. 1880-1860 Ma; Cliff et al., 1990; Romer et al., 1994; Wanhainen et al., 2005; Smith et al., 2007, 2009; Westhues et al., 2016; Martinsson et al., 2016), however

https://doi.org/10.5194/egusphere-2022-1475
Preprint. Discussion started: 9 January 2023

increasing structural evidence links a generation of Cu ± Au mineralization to brittle structures constrained to a late phase of the tectonic evolution (Bauer et al., 2018, 2022; Andersson et al., 2020, 2021), supported by radiometric studies (Storey et al., 2007; Martinsson et al., 2016; Sarlus et al., 2018; Andersson et al., 2022). These findings raise an important question about the relative timing of Cu ± Au introduction and/or remobilization in the Norrbotten ore province and how IOA mineralizing systems are related to Cu-Au occurrences in the context of the tectonic evolution. A well-characterized regional structural framework offers a tool for unraveling the relative timing of events where multiple generations of similar alteration and mineralization styles may overprint each other, where isotopic systems used for radiometric dating are subject to disturbance, or where datable phases in relevant textural positions are lacking.

In the southern Kiruna mining district, structurally and lithologically controlled, stratabound to discordant Cu ± Au deposits are known in the Pahtohavare area (Martinsson et al., 1997a) and occur ca. 2 km northwest of the Rakkurijärvi iron oxide-copper-gold (IOCG) deposit. These Fe ± Cu ± Au deposits are situated 5 km SW of the world-class Kiirunavaara IOA deposit which has received over a hundred years of scientific spotlight (e.g. Geijer, 1910; Lundbohm, 1910; Parák, 1975; Cliff et al., 1990; Cliff and Rickard, 1992; Nyström and Henriquez, 1994; Westhues et al., 2016) while the Fe ± Cu ± Au occurrences in the district have relatively few dedicated studies (e.g. Viscaria, Rakkurijärvi, Pahtohavare; Lindblom et al., 1996; Martinsson et al., 1997; Storey et al., 2007). Globally, there has been a growing interest in research on clarifying the genetic relationship between IOA and IOCG deposits. Several studies from the Chilean iron belt, the Great Bear Magmatic Zone, and the St. Francois Mountains terrane in SE Missouri argue that IOA and IOCG deposits form from a single evolving magmatic-hydrothermal or hydrothermal fluid during one ore-forming event (cf. Corriveau et al., 2016; Day et al., 2016; Barra et al., 2017; Simon et al., 2018), building on the concept that IOA deposits may represent the deeper roots of a spectrum between an IOA-IOCG mineral system (Sillitoe, 2003). However, other researchers argue that these two deposit types have distinct geneses despite sharing similar geologic environments and characteristics (e.g. Williams et al., 2005; Groves et al., 2010; Tornos, 2011; Barton, 2014; Martinsson et al., 2016; Skirrow, 2021). For example, some researchers favor a purely orthomagmatic model for IOA deposits (e.g. Nyström and Henriquez, 1994; Naslund et al., 2002; Velasco et al., 2016; Tornos et al., 2017; Troll et al., 2019); a model that is incongruous for some IOCG deposits in which a magmatic-hydrothermal fluid and/or metal source is indirect or ambiguous (c.f. Barton, 2014).

In this study, a structural investigation was conducted in the southern part of the Kiruna mining district where Cu ± Au occur with iron oxides (the Pahtohavare and Rakkurijärvi deposits) as a part of a broader mineral systems approach (Wyborn et al., 1994). The area is not significantly metamorphosed making it an optimal location for depiction of the structural context between IOA and IOCG-style mineralization. The structural results are constrained by a regional tectonic framework and used to illuminate the relative timing of the Pahtohavare Cu ± Au mineralization.

https://doi.org/10.5194/egusphere-2022-1475
Preprint. Discussion started: 9 January 2023

2 Geological Setting

The descriptions of the rocks used in this paper follows the nomenclature presented by Martinsson (2004). The rocks in northern Sweden are variably metamorphosed from greenschist to amphibolite facies conditions however, the "meta" -prefix is excluded for clarity and emphasis on the original protolith.

2.1 Regional geologic setting

2.1.1 Neoarchean buildup and early Paleoproterozoic rifting

The Norrbotten craton basement rocks comprise of Neoarchean (ca. 2.9-2.6 Ga) gneissic granitoids of tonalitic to granodioritic composition, amphibolites, and paragneisses (Martinsson et al., 1999; Bergman et al., 2001) which formed during the continental build-up of the Lopian orogeny (Bergman et al., 2001). The southwestern boundary of the Archean crust has been traced using εNd values in Paleoproterozoic plutonic-volcanic rocks (Öhlander et al., 1993) that broadly define the margin as running from the Bothnian Bay south of Luleå, towards the NW through Jokkmokk, hence, the Luleå-Jokkmokk line (Mellqvist, 1999; Fig. 1).

The early Paleoproterozoic marked major rifting events of the basement (ca. 2.5-2.0 Ga) which generated tholeiitic volcanic and volcaniclastic rocks and rift-related sedimentary successions forming a greenstone belt that extends today from northern Norway to Russian Karelia (Pharaoh and Pearce, 1984; Martinsson, 1997; Bingen et al., 2015). The greenstone successions are important hosts for syn- to post-depositional Fe, Cu, and Cu ± Au mineralization regionally (Martinsson et al., 2016).

2.1.2 Svecokarelian early orogenic extension and crustal shortening

Around 1.90 Ga, NE-directed subduction (BABEL Working Group, 1990; Öhlander et al., 1993) and back-arc extension (Pharaoh and Pearce, 1984; Andersson et al., 2021; Bauer et al., 2022) began along the southern margin of the Archean craton, marking the start of the polyphase Svecokarelian accretionary orogenic cycle (Bergman et al., 2001). Several magmatic events and associated deformation are recorded in the Norrbotten lithotectonic unit accompanied by varying degrees of hydrothermal alteration, metamorphism, and mineralization (c.f. Bergman et al., 2001; Martinsson et al., 2016; Grigull et al, 2018; Luth et al., 2018b; Bauer et al., 2018; 2022; Bergman and Weihed, 2020; Andersson et al., 2020; 2021). The resulting magmatic suites are the calc-alkaline to alkali-calcic Haparanda suite-Porphyrite group and Perthite monzonite suite (PMS)-Kiirunavaara group which vary from mafic to felsic rock types in the northern Norrbotten area (Perdahl and Frietsch, 1993; Bergman et al., 2001; Martinsson, 2004; Sarlus et al., 2020; Logan et al., 2022). Abundant Na-Ca metasomatism related to the elevated thermal flux from the intrusive activity and fluids channeling through faults resulted in the formation of albite, marialitic scapolite, magnetite, amphibole, and carbonate (Frietsch et al., 1997; Bergman et al., 2001; Martinsson et al., 2016; Andersson et al., 2020). The accretion of the Skellefte volcanic arc to the Archean craton to the north (Hietanen, 1975; Skiöld, 1988; Öhlander et al., 1993; Weihed et al., 2002; Bergman and Weihed, 2020; Skyttä et al., 2020) resulted in crustal shortening from ca. 1.88-1.86 Ga (termed D1 in Norrbotten, but D2 in the Skellefte district and Överkalix lithotectonic unit; Skyttä et al., 2012; Bergman

https://doi.org/10.5194/egusphere-2022-1475
Preprint. Discussion started: 9 January 2023

and Weihed, 2020). Structurally, the event is characterized by a penetrative tectonic fabric development from an inferred NE-SW shortening direction under mostly plastic conditions (Grigull et al., 2018; Bauer et al., 2018, 2022; Andersson et al., 2020, 2021). The fabric is interpreted to have formed under peak metamorphic conditions (lower amphibolite) recorded by syn-tectonic growth of hornblende (Andersson et al. 2020), though regionally the metamorphic grade can be higher (Bergman et al., 2001). Amphibolite facies metamorphism characterizes M1 in Norrbotten except in the Kiruna mining district which shows a lower overall metamorphic grade characterized by upper greenschist facies metamorphism (Bergman et al., 2001, Andersson et al. 2021; 2022). In the Skellefte district a 1.87 Ga basin inversion is observed (Bauer et al., 2011; Skyttä et al., 2012), however, it is not recorded or is masked in the Kiruna mining district (Andersson et al. 2021).

2.1.3 Svecokarelian late orogenic crustal shortening

A second phase of subduction initiated around 1.81-1.78 Ga, coeval with abundant crustal melting and emplacement of silica-rich granites of the Lina suite and quartz-poor monzonitic A-/I-type granitoids, syenites, and gabbros of the Transscandinavian Igneous Belt (Bergman et al., 2001; Högdahl et al., 2004; Bergman et al., 2006; Martinsson et al., 2018; Sarlus et al., 2018). Metamorphism has been suggested to be of high temperature, low pressure conditions during this orogenic phase (Bergman et al., 2001; Bauer et al., 2018). Commonly, K to K-Fe metasomatism/alteration can be found in late orogenic (D2) shear zones and brittle fractures (Andersson et al, 2020; Bauer et al., 2022) and occurs in spatial proximity to late orogenic intrusions and pegmatites or as a result of late magmatic-hydrothermal activity (Andersson et al, 2020; Bauer et al., 2018; 2022). The second deformation event resulted from E-W crustal shortening (e.g. Bergman et al., 2001; Weihed et al., 2002; Lahtinen et al., 2005; Bauer et al., 2018; Luth et al., 2018b; Andersson et al., 2021) and is associated with brittle-plastic conditions producing spaced S_2 cleavages and strong strain partitioning (Grigull et al., 2018, Luth et al., 2018b, Bauer et al., 2018; 2022, Andersson et al, 2020). This was followed by a clockwise-rotation of the stress field to a NNW-SSE- to N-S-oriented crustal shortening direction (D3) which caused a gentle refolding of preexisting fabrics and crenulation of white mica and chlorite domains recorded in the Kiruna area (Andersson et al. 2021). A similar direction of crustal shortening related to D3 is recorded in the Pajala area to the east, however it differs from that seen in Kiruna by the resultant formation of conjugate faults (Luth et al., 2018a).

2.1.4 Late Svecokarelian

A late brittle deformation event is observed in the Kiruna and Gällivare areas (Romer, 1996; Bauer et al., 2018; Andersson et al., 2021). At the Luossavaara and Rektor IOA deposits, a calcite-quartz hydraulic breccia cross cuts S_2 fabrics (Andersson et al., 2021). Furthermore, a late hydrothermal event is identified by radiometric age constraints on monazite from the Rektor and Kiirunavaara ores which yield U-Pb ages of ca. 1.74-1.72 Ga and ca. 1.62 Ga (Blomgren, 2015, LA-ICP-MS; Westhues et al., 2017, SIMS). U-Pb (SC-ICP-MS) ages from monazite in hydrothermal calcite found in the Kiruna Naimakka shear zone in central Kiruna show formation at ca. 1.78-1.76 Ga (Lauri et al., 2022). At Malmberget in the Gällivare area, low-temperature hydrothermal monazite and stilbite associated to late calcite-bearing brittle fractures yield U-Pb crystallization ages between

https://doi.org/10.5194/egusphere-2022-1475
Preprint. Discussion started: 9 January 2023

ca. 1.74-1.73 Ga with associated apatite and titanite showing a later recrystallization and/or hydrothermal event around ca. 1.60-1.62 Ga (ID-TIMS, Romer 1996).

2.2 Local geology

2.2.1 Stratigraphy and intrusive rocks

The Kiruna mining district, outlined in Fig. 2, has a well-preserved stratigraphy which has been comprehensively described by Lundbohm (1910), Frietsch et al. (1979), Martinsson et al. (2004), and Andersson et al. (2021). A small occurrence of Archean granite outcrops in the southern part of the district and is overlain unconformably by greenstone stratigraphy and later Orosirian rocks (Martinsson, 1997). The lowermost succession of greenstones belongs to the ca. 2.5-2.3 Ga Kovo group, comprising basal clastic sedimentary rocks, basaltic lavas, volcanogenic graywackes, and a series of tholeiitic to calc-alkaline volcanic rocks (Martinsson 1997). Above this unit lies the Kiruna greenstone group which consists of basaltic lavas, conglomerates, and dolostones at the base that transitions into komatiitic to tholeiitic volcanics, tholeiitic to calc-alkaline volcanosedimentary formations, graphite schists, and pillow basalts with related mafic sills within the volcaniclastic unit (Martinsson 1997).

The mid-Orosirian rocks related to the early-Svecokarelian orogenic cycle overlie the greenstones with the unconformable Kurravaara conglomerate at the base. This unit is polymictic, poorly sorted, with rounded to subrounded clasts approximately 0.5 to >10 cm (locally up to 50 cm) in size (Frietsch, 1979). A volcanic intercalation in the Kurravaara conglomerate has been radiometrically dated (U-Pb zircon SIMS), which constrains the minimum age of the conglomerate to ca. 1.89 Ga (Andersson et al., 2021). In some areas, andesitic volcanic rocks of the Porphyrite group are the lowermost unit of the Orosirian stratigraphy, and represent the extrusive products of early arc magmatism (Martinsson and Perdahl, 1995; Martinsson, 2004). Overlying these basal units are the volcanic rocks of the Kiirunavaara group including the trachyandesitic Hopukka formation and dacitic-rhyolitic Luossavaara formation which make up the footwall and hanging wall, respectively, to the giant Kiirunavaara IOA deposit (Martinsson 2004). Above the Luossavaara formation are a series of rhyolitic tuffs, basaltic lavas, alluvial breccia-conglomerates, greywackes and phyllites of the Matojärvi formation (Lundbohm, 1910; Frietsch, 1979; Martinsson, 2004; Andersson et al., 2021) which represents a highly tectonized unit of the stratigraphy (Andersson et al., 2021). This formation is overlain by quartz-feldspar arenites with intercalations of alluvial breccia-conglomerates forming the Hauki quartzite (Lundbohm 1910, Martinsson 2004).

Distributed through the Kiruna mining district are mafic to felsic plutonic intrusions (Offerberg, 1967) regarded as comagmatic with the Kiirunavaara group volcanic rocks and suggested to belong to the PMS (Witschard, 1984; Martinsson, 2004). Radiometric dating (U-Pb zircon by ID-TIMS and SIMS) of these intrusions verifies an early orogenic timing (ca. 1.90-1.86 Ga) of magmatic activity (Cliff et al., 1990; Westhues et al., 2016; Logan et al., 2022). Only one U-Pb radiometric determination (ID-TIMS zircon and titanite) has indicated a late orogenic age for a syenitic intrusion in the district (Romer et

https://doi.org/10.5194/egusphere-2022-1475
Preprint. Discussion started: 9 January 2023

al., 1994); however recent geochronological work from the area could not confirm the timing, making the presence of a late orogenic intrusive body enigmatic (Logan et al., 2022).

Structurally, the Kiruna mining district is affected by several periods of tectonic activity. The earliest direct age determination on deformation in the district comes from fracture plane-hosted hydrothermal titanite in a cataclastic fault damage zone at Luossavaara showing the minimum age of fault initiation to be 1889 ± 26 Ma (Andersson et al., 2022). This is interpreted to represent syn-volcanic faulting during the basin evolution of the early Svecokarelian. In the southern Kiruna mining district, the Rakkurijärvi IOCG deposit is situated adjacent to a NE-SW trending fault zone that controls the mineralization (Smith et al., 2007). The deposit was dated (Re-Os molybdenite and U-Pb LA-ICP-MS allanite, U-Pb TIMS rutile) to have formed around 1.86 Ga (Smith et al., 2007; 2009; Martinsson et al., 2016) and suggests the fault was active during the early orogenic crustal shortening period of the Svecokarelian. The Orosirian portion of the central Kiruna area is reported to lack early orogenic (D1) deformation fabrics and predominantly records late orogenic (D2) E-W crustal shortening and basin inversion between 1812 ± 3 Ma and 1802 ± 8 (Andersson et al., 2021, 2022). Generally east-side-up kinematics are recorded which are similarly observed in the Kiruna Naimakka deformation zone that runs approximately 5 km to the east of Kiruna (Luth et al. 2018b, Andersson et al. 2021), but contrasting kinematics further north have also been reported (Bergman et al. 2001).

2.2.2 Local ore deposits

The Kiruna mining district is host to Kiruna-type IOA deposits and a variety of Cu-mineralization including stratiform-stratabound Cu (Fe-Zn) deposits (i.e. Viscaria, Eastern Pahtohavare; Martinsson et al., 1997b), epigenetic stratabound to discordant Cu ± Au deposits (Southern, Southeastern, and Central Pahtohavare; Martinsson et al., 1997a), and IOCG-style deposits (Rakkurijärvi; Smith et al., 2007). While different genetic models exist, thorough structural assessments for the copper deposits are lacking.

The area is best known for the giant Kiirunavaara IOA deposit that has been actively mined for iron ore for over a century (Fig. 2). The deposit is a tabular body of low-Ti magnetite-apatite ore with brecciated hanging and footwall contact zones (Geijer, 1919; Bergman et al., 2001; Martinsson and Hansson, 2004) and is situated along the lithological contact between the Hopukka and Luossavaara formations. U-Pb radiometric data constrain the timing of the ore formation through the dating of host rocks, ore minerals, and alteration minerals to ca. 1880 Ma (Welin, 1987; Cliff et al., 1990; Romer et al., 1994; Smith et al., 2009; Westhues et al., 2016; Martinsson et al., 2016). However, only recently has the structural context of the ore-system been incorporated into a genetic model, with the emplacement of IOA deposits suggested to be coeval with syn-volcanic faulting during early orogenic basin development and back arc extension (Andersson et al., 2022).

The Rakkurijärvi deposits (ca. 1.86 Ga; Smith et al., 2007; 2009; Martinsson et al., 2016) occur spatially associated to a NE-SW trending shear zone approximately 5 km SSE of the Kiirunavaara IOA (Fig. 2) and have been described to be IOCG deposits (Smith et al., 2010). The ore bodies occur in both the Kurravaara conglomerate and in the Kiirunavaara group volcanics (Smith et al., 2007). Chalcopyrite is the main ore bearing sulfide which was precipitated with calcite in the matrix of brecciated massive magnetite and of lithic breccias (Smith et al., 2007). Selective-pervasive magnetite replacement of

https://doi.org/10.5194/egusphere-2022-1475
Preprint. Discussion started: 9 January 2023

conglomerate clasts and Cu mineralization within the Kurravaara conglomerate suggests some mineralization is a product of hydrothermal replacement (Smith et al., 2007).

The deposits at Pahtohavare (four sub-localities: Southern, Southeastern, Central, and Eastern) are situated in the Kiruna greenstone group approximately 5 km SW of the Kiirunavaara IOA. The host stratigraphy is folded into a southeast-plunging anticline and truncated on the southwest by a NW-SE trending shear zone (Fig. 2). The earliest mineralization (Eastern Pahtohavare) is suggested to have formed during the deposition of the greenstones (ca. 2.1 Ga) in an exhalative environment based on the stratiform character, alteration in the footwall, and Cu/Zn zonation (Martinsson et al., 1997b). The ore bodies at Southern, Southeastern, and Central are considered epigenetic and are both structurally and lithologically controlled (Martinsson et al., 1997a). Southern and Southeastern Pahtohavare were mined over a period of seven years during the 1990's and produced 1.7 Mt of ore with 1.9% Cu and 0.9 ppm Au (Martinsson et al., 1997a), while the ore body at Central is unmined and dominated by secondary oxidized mineral assemblages. The ore minerals at Southern and Southeastern consists of chalcopyrite and pyrite which occur both disseminated and as breccia infill in albite-altered graphite schist and tuffite horizons. Pyrite-chalcopyrite also occur in veins of quartz-carbonate in the ore zone. Occasionally thin magnetite-rich horizons occur within the hosting tuffites (Lindblom et al., 1996; Martinsson et al., 1997a). The age of the Pahtohavare deposit has not been determined radiometrically, however, it has been suggested to be of a similar age as the Rakkurijärvi deposit (Martinsson et al., 2016).

3 Methods

3.1 Geologic mapping and sampling

Geologic mapping and structural analysis were carried out between 2019-2021. Approximately 280 field measurements were taken from 129 localities in the Kiruna mining district using a Breithaupt Kassel compass. Structural measurements are reported using the dip/dip azimuth and plunge/azimuth conventions. For magnetite-rich rocks, sighting measurements guided by known points in the terrain were made with the compass to reduce magnetic-induced errors. Measurements were digitized directly in the field using the Field Move application (Petroleum Experts Ltd.) on a ruggedized iPad Mini device. Subsequent structural analyses were performed in the software Move (Petroleum Experts Ltd.).

Sampling was conducted in the field and from drill core at the Geological Survey of Sweden's National Drill Core Archive in Malå. Thirty-seven thin sections were prepared by Precision Petrographics Ltd. in Vancouver in Canada for petrographic and structural investigation.

3.2 3D Modeling

The Pahtohavare-Rakkurijävi area is relatively less explored compared to the central Kiruna area and the available observations and measurements are concentrated around the closed open-pit areas. The geological model incorporates the structural measurements and the geological map from this study, a digital elevation model based on Läntmateriet elevation data (2+m

https://doi.org/10.5194/egusphere-2022-1475
Preprint. Discussion started: 9 January 2023

grid precision), and drill hole lithological logs from 31 holes (open-source data from the Swedish Geological Survey). In total 6625m of drill cores were available with an average depth of 214 m. Drill cores were not oriented, therefore structural measurements were not available.

A surface-based modeling approach was applied to build a three-dimensional geological model of the Pahtohavare-Rakkurijärvi area, with the aim to facilitate the visualization and understanding of the lithological and structural framework of the area. The horizontal extent of the model shares the boundaries with the geological map (Fig. 3) and has a vertical range of 1000 m. The vertical range of the model was selected due to the scale of the well-known structures further north in the central Kiruna area and the open end of the structures from the shallow drillholes. A combination of explicit and implicit 3D geomodelling was utilized in Leapfrog Geo (version 2021.2.4, by Seequent). Surface structural measurements were used as implicit, primary indicators for bedding orientations and the dips were estimated from the continuation of lithological units that were traced through several drillholes. Contacts of lithological units were implemented explicitly by tracing the lithological boundaries from the geological map and drillhole sections.

4. Results

4.1 Structural analysis

The study area is located approximately 5 km south-southwest of the Kiirunavaara IOA deposit and hosts the Pahtohavare and Rakkurijärvi deposits (Fig. 3). The rocks in the area are folded into a SE-plunging anticline and is structurally bound to the east and southwest by shear zones trending NE-SW and NW-SE, respectively. From Pahtohavare, a relatively well-exposed ridgeline runs parallel to the axial trace of the anticline (Fig. 3) and flattens into swampy terrain towards the Rakkurijärvi area. A lower hemisphere, equal area stereographic projection of bedding planes (Fig. 3A) indicates that the geometry of the fold is non-cylindrical with a subvertical to inclined axial plane, and is moderately SE plunging (34/149 fold axis). The spatial distribution of bedding dip directions within the fold limbs are somewhat irregular, and may reflect parasitic folding, a feature that is clearly observed in outcrop at the Pahtohavare Southern open pit (Fig. 4A).

An important observation in the Pahtohavare area is the occurrence of two distinct fabrics. A bedding-subparallel tectonic fabric is observed both in outcrop and in thin section. The bedding-subparallel fabric in thin section shows a mylonitic texture containing porphyroclasts with recrystallized strain shadows (Fig. 4B-F). It is well developed in rheologically weak units such as in pyroclastic layers and graphite schists. In certain samples, this fabric is overprinted by a spaced cleavage (Fig. 4B-D). Another example of two distinct fabrics is shown by preserved foliation trails in a scapolite porphyroblast which are discordant to the foliation that wraps around it (Fig. 4G). Additionally, in the Saarijärvi area, two separate fabrics are observed affecting granitic intrusions (Fig. 4H).

The cleavage measurements from the Pahtohavare-Rakkurijärvi area show an overall similar folding pattern as the bedding (Fig. 3B), with the fold axis of the foliation occurring steeper than the that of the bedding (β = 69/163). To account for possible bias from misclassification of bedding versus bedding-subparallel cleavage measurements during mapping, Figure 3C shows

https://doi.org/10.5194/egusphere-2022-1475
Preprint. Discussion started: 9 January 2023

the combined bedding and cleavage measurements which illustrate a folding pattern consistent with the geometry depicted by the bedding and the map trace of the fold.

Plotted together in the stereographic projections are a fold axis and axial planar fabric of a local parasitic fold from the Pahtohavare Southern open pit (purple pole and gray great circles, Fig. 3B-C), which illustrate how folding patterns can locally deviate from the overall orientation of the fold. The parasitic fold shows evidence for bedding-subparallel foliation defined by biotite and scapolite. Furthermore, scapolite veins mimic the orientation of the axial plane parallel cleavage suggesting vein injection during late tectonic processes (Druguet, 2019), consistent with brittle-plastic conditions associated to the late phase of the Svecokarelian orogeny (Andersson et al, 2020; 2021; Bauer et al., 2022,). The combined structural, outcrop, and thin section observations indicate the fold in the Pahtohavare-Rakkurijärvi area is an F_2 fold formed under non-coaxial strain, and that both S_1 and S_2 fabrics are preserved.

Importantly, quartz-carbonate ± pyrite ± chalcopyrite veins, a main ore-related mineral assemblage for the epigenetic Pahtohavare deposits, cross cut tectonic cleavage at the Southern Pahtohavare open pit (Fig. 4I). These veins show both brittle and plastic deformation manifested by small-scale syn-tectonic shear bands and brittle fractures. One small-scale (10 cm wide) quartz-carbonate ± pyrite ± chalcopyrite shear band mirrors the orientation of the NW-SE trending shear zone (80/065) and a mineral lineation defined by scapolite (55/162) on the foliation plane shows a moderate oblique-reverse movement. An oriented thin section from this shear zone indicates a sinistral sense of shear and NE-side up kinematics (Fig. 4J-K). The quartz-carbonate ± pyrite ± chalcopyrite vein orientations from the Southern Pahtohavare open pit are plotted in Fig. 3D with orientations either sub-parallel with- or off-axis to the axial plane. The data suggest that veining (and subsequent alteration and mineralization) occurred syn- to post- F_2 folding in response to sinistral oblique-reverse movement and indicate that the Pahtohavare epigenetic Cu ± Au deposits can be structurally-constrained to the late Sveockarelian orogeny.

The outcrops near the Rakkurijärvi shear zone record a transposition of fabric into the NE-SW orientation of the shear zone (Fig. 3E). Tensional gashes and brittle fracturing record tensile openings with a NW-SE orientation. Strain intensity abruptly decreases with distance from the shear zone, and strain partitioning effects are common in outcrop-scale throughout the study area (Fig. 4L). On the SE side of the shear zone, the greenstone stratigraphy occurs as a tectonically displaced unit, a feature that is also observed in the central Kiruna area (Offerberg, 1967).

4.2 Geological model

A 3D geological model generated based on drill hole data and the geological map (Fig. 3) visualizes the main lithological boundaries and structures for the study area (Fig. 5). The relatively shallow drill holes (down to 300 m), indicate a complex intercalation between gabbro, graphitic schist, hornblendite, chert, and greenstones composed mainly of basaltic tuff. Based on the lithological logs from the drill cores, the markers were grouped in four units: graphite schist, gabbroic sill, pillow basalts and undifferentiated greenstones. The trachyandesitic Hopukka formation, andesitic Porphyrite group, igneous granite-syenite of the PMS, and the Kurravaara conglomerate were not intersected by the selected drill holes and were traced based on the map extent to constrain the model. Faults were added based on the geological map (illustrated in red in Figure 5) and were

https://doi.org/10.5194/egusphere-2022-1475
Preprint. Discussion started: 9 January 2023

modeled as hard boundaries that separate fault blocks. Two perpendicular conceptual cross-sections were created based on the geological model (AA` and BB` in Figure 5) and contain additional interpretations for an improved visualization of the crustal architecture, illustrating the SE plunging anticline and the relationship between the lithostratigraphic units. The conceptual cross sections highlight the geometry of the fold showing a curvilinear fold axis and moderate plunge to the SE (Fig. 5A AA'). The anticlinal nature with a subvertical axial plane which trends subparallel to the NW-SE shear zone is seen in Figure 5B (BB'). Furthermore, it illustrates the interplay between the major shear zones and secondary fault structures that show minimal offset but are interpreted to have formed as a result of brittle-plastic noncoaxial strain between the two conjoining shear zones. The NW-SE oriented shear zone truncates the southwestern limb of the Pahtohavare fold and probably played an important role in controlling the shape of the fold during the deformational events.

5. Discussion

Clarifying the degree of Cu-Au mineralization associated to each stage (early and late) of the Svecokarelian orogeny in Norrbotten is critical for understanding the mineral systems and the relationships between IOA and IOCG deposits. However, overprinting deformation, metamorphism, magmatism, and alteration complicate interpretation of vectors to ore and the identification of ingredients of the different mineral systems. Some Cu-Au mineralization in Norrbotten has been linked to the early Svecokarelian orogeny (e.g. Aitik porphyry Cu (Au-Ag-Mo) deposit, Rakkurijärvi IOCG; Wanhainen et al., 2012; Smith et al., 2007), but a significant contribution of Cu-Au occurs as late-orogenic overprints (e.g. IOCG-overprint at Aitik and the Nautanen deformation zone as well as at the Malmberget and Gruvberget IOA deposits; Wanhainen et al., 2012; Martinsson et al., 2016; Bauer et al. 2018; Bauer et al., 2022). Therefore, assessing energy drivers, fluid and metal sources, transport pathways, and traps (Wyborn et al., 1994) by framing them within the tectonic framework is useful for unraveling complicated and overprinted relationships. Bauer et al. (2018, 2022) use structural constraints on alteration and mineralization indicating Cu-Au mineralization in the Nautanen deformation zone and the Malmberget IOA deposit are hosted in late orogenic structures, and they suggest that either a late mineralization with new metal input occurred, or that tectonically late structures acted as traps for remobilized metals. The question of which mineralized deposits are associated to each phase of the Svecokarelian orogeny and whether these represent unique mineralization events remains an important factor in understanding IOA and IOCG genetic relationships in northern Norrbotten. Below, the Kiruna mining district ore forming processes are temporally placed within the context of the tectonic framework and transport pathways and traps of the mineral systems are discussed.

5.1 Timing of ore forming processes

Structural analysis of the Pahtohavare-Rakkurijärvi area gives critical insight into the timing of ore formation for the epigenetic Pahtohavare Cu ± Au deposits. The structural characterization of the northern Norrbotten ore province defines two major periods of fabric development during the tectonic evolution. Regionally, S_1 reflects an inferred NE-SW crustal shortening

https://doi.org/10.5194/egusphere-2022-1475
Preprint. Discussion started: 9 January 2023

which formed a regionally distributed and penetrative, yet heterogeneously developed fabric (Bergman et al., 2001, Grigull et al., 2018, Bauer et al., 2018, Andersson et al., 2020, Bauer et al., 2022). S_2 records an inferred E-W crustal shortening forming a spaced fabric (Luth et al., 2018b, Grigull et al., 2018, Bauer et al., 2018, 2022, Andersson et al., 2020, 2021). A similar structural pattern is observed in the bedrock in the southern Kiruna district. A bedding-subparallel foliation is best observed in rheologically, relatively weak rocks and asymmetric sigmoidal clasts with recrystallized pressure shadows indicate tectonic non-coaxial strain occurred during formation. The pressure shadows exclude that the fabric formed from compaction foliation along bedding, though the presence of compaction foliation in the shallower Orosirian part of the stratigraphy (Andersson et al., 2021) suggests the tectonic fabric probably overprinted (or occurred simultaneously to) a compaction fabric in the Rhyacian and lower Orosirian rocks. The bedding-subparallel foliation is here interpreted as S_1. Given the subparallel orientation to bedding of the tectonic S_1 and the correlating folding pattern of the bedding and cleavage measurements (Fig. 3B-C), the anticline in the Pahtohavare-Rakkurijärvi area can be constrained as an F_2 fold resulting from late Svecokarelian orogenic deformation. In thin section, the S_2 foliation is observed occurring as spaced cleavage and axial planar to parasitic F_2 folds (Fig. 4B-C), a characteristic also seen regionally (Luth et al., 2018b, Grigull et al., 2018, Andersson et al., 2020, Bauer et al., 2022). Both S_1 and S_2 cleavage data are likely represented in Figure 3B-C, however, without observations of cross cutting relationships in the field, the separate generations were not divided on the stereographic projection. However, S_2 cleavage is presumed to trend subparallel with the axial plane of the F_2 fold.

Importantly, in the Southern Pahtohavare open pit, ore-related quartz-carbonate ± pyrite ± chalcopyrite veins and narrow (10-20 cm wide) shear bands are observed cutting an earlier tectonic foliation (Fig. 4I). In the shear bands, quartz-ferrodolomite-calcite-pyrite-chalcopyrite mineral assemblages are boudinaged and infiltrate along folded bedding planes which reflect plastic behavior during syn-tectonic emplacement, likely coeval to the folding. However, the orientation of the veins varies from axial plane parallel to orientations at an angle to the axial plane (Fig. 3D), utilizing tensional fractures during shearing and folding which comparatively indicates brittle-plastic conditions. Previous documentation of Southern and Southeastern Pahtohavare has described the deposits are structurally controlled especially in structures at an angle to the fold hinge (Martinsson et al., 1997a). In the absence of a regional tectonic framework and geochronological constraints, the timing of the epigenetic Pahtohavare deposits was unknown but suggested to be of similar age as the Rakkurijärvi IOCG deposit, for which radiometric age data (Re-Os molybdenite, U-Pb LA-ICP-MS allanite, U-Pb TIMS rutile) indicate formation at ca. 1.86 Ga (Smith et al., 2007, 2009; Martinsson et al., 2016). However, the results of the structural investigation and the designation of the Pahtohavare fold as F_2 allows the Pahtohavare epigenetic deposits to be assigned to the late Svecokarelian mineral system, which in Kiruna is constrained by syn-tectonic titanite data at ca. 1.81-1.79 Ga (Andersson et al. 2022). Furthermore, this illustrates that brittle-ductile, non-coaxial shear zones and resultant S_2 structures associated to the E-W-oriented late orogenic deformation served as pathways for ore fluids. In the Pahtohavare area, traps for the mineral system likely occur where these pathways intersected favorable reducing horizons of graphitic schist, which has been shown to be an important lithological trap for the ore (Martinsson et al., 1997a). The structural results from this study are the first to show a late-Svecokarelian timing for Cu ± Au mineralization in the Kiruna mining district.

https://doi.org/10.5194/egusphere-2022-1475
Preprint. Discussion started: 9 January 2023

5.2 Structural framework in Kiruna

The structural framework of the Kiruna mining district presents ambiguities in context of the regional tectonic evolution. While an S_1 fabric is observed regionally (Bergman et al., 2001, Grigull et al., 2018, Bauer et al., 2018, Andersson et al., 2020, Bauer et al., 2022), in the Kiruna mining district it is absent or masked in the structural data obtained from the Orosirian part of the stratigraphy (Andersson et al., 2021). Subsequently, Andersson et al. (2021) suggested the central Kiruna area represents a higher crustal level that was too shallow to have experienced plastic deformation during the early orogenic phase. Furthermore, structural evidence shows that blocks of lower crustal levels were uplifted with reverse west-side-up kinematics along steep west-dipping structures southeast and west of Kiruna (Lynch et al., 2015; Andersson et al., 2020) and with reverse east-side-up kinematics to the east and northeast along east-dipping structures (Luth et al., 2018b, Andersson et al., 2021). Other structural investigations have noted that the Kiruna area records fewer folding phases compared to the regions to the north and east (Vollmer et al., 1984; Grigull et al., 2018; Luth et al., 2018b).

The results of the current study document the presence of an S_1 tectonic fabric in the bedrock that underlies the Orosirian sequence (Kiruna greenstone group and Kurravaara conglomerate) around Pahtohavare, Rakkurijärvi, and Saarijärvi (Fig. 2-3). In addition to the pressure shadows on porphyroclasts and mylonitic bedding-subparallel fabric observed in thin section (Fig. 4B-F), the presence an early S_1 fabric in a scapolite porphyroblast (Fig. 4G) and of two generations of tectonic fabric in granitic intrusions in the southern part of the district (Fig. 4H) excludes that the foliation is from compaction alone. Evidence of S_1 (or S_0/S_1) and S_2 fabrics is also noted in a previous mapping campaign in the Saarijärvi area (Martinsson et al., 1993). The current study indicates that the deeper stratigraphy belonging to the Rhyacian and lower Orosirian rocks in the southern Kiruna mining district were affected by a tectonic foliation-forming event while the higher Orosirian rocks in the central Kiruna were not. Possible explanations for this discrepancy are that the fabric developed heterogeneously in response to shearing and/or an elevated geothermal gradient. Shear foliation could account for the locally and heterogeneously developed tectonic fabric in the greenstones sequence (e.g. graphite schists, pyroclastic tuffs, mafic sills, e.g. Fig. 4B-F, 4I). However, the two generations of foliation in competent rocks (e.g. granitic outcrops in the southern part of the district, Fig. 4H) calls for ductile deformation possibly explained by a locally elevated geothermal gradient in this area. Logan et al. (2022) recently conducted U-Pb zircon geochronology on several intrusions in the southern part of the district that showed a dominantly early Svecokarelian timing for the magmatism. The abundant magmatism would have resulted in increased fluid circulation and may have facilitated the heterogenous formation of a ductile S_1 fabric. Extensive hydrothermal fluid flow driven by abundant igneous activity has been postulated as an explanation for the regional style Na-metasomatism (e.g. scapolite and albite), which is also restricted to large-scale shear zones (Frietsch et al., 1997; Bergman et al., 2001). In the central Kiruna area the regional-style scapolite alteration occurs more rarely (Bergman et al., 2001, Martinsson 2004), and the Na-Ca (+ Fe ± Cl) and alkali alteration styles recorded are spatially associated to local IOA deposits (Martinsson, 2015; Martinsson et al., 2016).

A conceptual framework of the structural evolution of the Kiruna area is proposed in Figure 6 which synthesizes the structural results presented in this paper with those produced by Andersson et al. (2021), and is also based on previous structural mapping

https://doi.org/10.5194/egusphere-2022-1475
Preprint. Discussion started: 9 January 2023

from the Kiruna area (Wright, 1988; Martinsson et al., 1993; Grigull et al., 2018) as well as the Geological Survey of Sweden's magnetic anomaly map of the district (Bergman et al. 2001). This framework is offered as a working model and can be subject to modification with future work in the district. The NW-SE-trending shear zone to the southwest of the fold in the Pahtohavare-Rakkurijärvi area, here referred to as the Pahtohavare shear zone, is interpreted to be a reactivated early normal fault structure. This structure formed during the back arc extension of the early Svecokarelian orogeny (Fig. 6A), or possibly even earlier during the Rhyacian rifting. Upon the early NE-SW oriented crustal shortening at ca. 1.87 Ga (Fig. 6B), the structure reactivated with reverse kinematics and an early tectonic S_1 fabric was heterogeneously developed, possibly forming as a shear foliation and/or as a result of a locally elevated geothermal gradient. At the same time, the NE-SW to N-S structure that runs adjacent to the Rakkurijärvi deposit and through central Kiruna (Fig. 2-3), would have responded with oblique reverse shearing (Fig. 6B) and offered conduits along which ore fluids could transport. During the E-W brittle-plastic crustal shortening of the late Svecokarelian orogeny, extensive reactivation of fault systems occurred in the Kiruna mining district (Fig. 6C). Basin inversion manifested from the crustal shortening (Andersson et al., 2021) and strong strain partitioning occurred, forming high strain fabrics along shear zones, and spaced- to heterogeneously-developed fabric outside of these zones. Conjugate faulting subparallel to the E-W shortening direction occurred in response to the stress direction. The Pahtohavare shear zone responded with sinistral reverse-oblique kinematics causing vertical extrusion of the rocks and non-cylindrical anticlinal folding. This juxtaposed the older Rhyacian volcanic rocks to the northeast with younger Orosirian volcanic rocks on the southwest (Fig. 3, 7). During this time the brittle-ductile strain created tensional structures for ore fluids to propagate through in the Pahtohavare area. Finally, at ca. <1.79 Ga (cf. Andersson et al., 2022), a N-S oriented crustal shortening led to gentle refolding (Andersson et al., 2021) and minor reactivation of preexisting fault structures (Fig 6D).

5.3 Implications for the Kiruna mining district mineral systems and relationships between IOA and IOCG mineralization

This study shows that multiple mineralization events in the Kiruna mining district can be linked to specific phases of the tectonic evolution. Using the proposed structural framework presented in Figure 6, the timing of mineralization within a structural context can be synthesized. The earliest mineralization known in the district (e.g. Viscaria and Eastern Pahtohavare) has been suggested to have occurred syngenetically during deposition of the Kiruna greenstone group around ca. 2.1 Ga from Rhyacian rifting (Martinsson et al., 1997a, b). Following this mineralization and rifting period, during the Orosirian back arc extension and basin development in the district, the development of syn-volcanic normal and transtensional faults (Fig. 6A) occurred around 1889 ± 26 Ma (Andersson et al., 2022), shown by in situ U-Pb (LA-ICP-MS) dating of titanite in a hydrothermally altered damage zone to a fault system associated with the Luossavaara IOA deposit. Such a timing is coeval with volcanism in the district as well as the accepted age for the IOA formation (1888 ± 6, U-Pb ICP-MS titanite; 1874 ± 7 Ma and 1877 ± 4 Ma, U-Pb SIMS zircon; 1878 ±4 Ma, U-Pb TIMS titanite; Romer et al., 1994, Westhues et al., 2016, Martinsson et al., 2016). It was therefore suggested that normal faulting in an extensional regime may have played an important role for the emplacement of the IOA ore (Andersson et al., 2022). Conversely, following the onset of crustal shortening (Fig.

https://doi.org/10.5194/egusphere-2022-1475
Preprint. Discussion started: 9 January 2023

6B), the Rakkurijärvi IOCG deposit formed and is described to be related to the NE-SW shear zone adjacent to the deposit (Smith et al., 2007), implying that the faulting activity was active around ore formation at ca. 1.86 Ga (Smith et al., 2007, 2009, Martinsson et al., 2016). Such a context supports that IOA and IOCG deposits may form within 20 Myr of each other as indicated in other classic IOCG-IOA terrains (e.g. the Chilean iron belt; c.f. Skirrow 2021 and references therein). It is possible that IOA and IOCG deposits share some mineral system ingredients, however, in Kiruna distinct tectonic regimes separate the formation of IOA and IOCG deposits respectively (Fig. 6A-C).

The establishment of a late orogenic timing for the epigenetic Pahtohavare Cu ± Au deposits indicates that a time gap of ca. 80 Myr or more exists between the younger episode of Cu ± Au mineralization and the IOA emplacement in the Kiruna mining district. The indicated time-gap introduces important implications for the current debates about IOA and IOCG genetic continuums (c.f. Reich et al., 2016; Corriveau et al., 2016; Barra et al., 2017; Simon et al., 2018; del Real et al., 2021) as the later Cu ± Au event in Norrbotten lacks clear temporal associations to IOA deposits; this is in line with the mineralization in the Cloncurry district in Australia where IOCG-style deposits occur without Kiruna-type IOA deposits (cf. Groves et al., 2010; Reich et al., 2022). Furthermore, in the Gällivare area, approximately 70 km southeast of Kiruna, two distinct mineralizing periods related to different phases of the tectonic evolution are also described. The Malmberget IOA deposit is considered to have formed during the early orogenic phase (ca. 1.89-1.88 Ga), constrained by the age of the host rocks (Sarlus et al., 2020) and from structural analysis showing the iron ore was affected by two deformation events (Bergman et al., 2001, Bauer et al., 2018). Late IOCG-style mineralization is suggested to have overprinted the area around 1.80 Ga at Aitik (Wanhainen et al., 2012) as well as in the Nautanen deformation zone where mineralization is also situated in late orogenic structures (Bauer et al., 2022). From a mineral systems perspective, multiply-reactivated structures (e.g. Fig. 6) may play an important role for fluid and transport pathways even if IOA and IOCG-style mineralization can be separated in time and by tectonic regimes. For example, the N-S to NE-SW trending structure adjacent to the shear zone-controlled Rakkurijärvi IOCG deposit (Fig. 2, 3) can be constrained by radiometric age determinations (ca. 1.86 Ga; Smith et al., 2007; 2009; Martinsson et al., 2016), but has also been shown by structural analysis to be active during the late Svecokarelian orogeny (ca. 1.81-1.79 Ga; Andersson et al., 2021, 2022). Furthermore, U-Pb (SC-ICP-MS) ages from monazite in hydrothermal calcite found within the same shear zone in central Kiruna show that the structure was again active at ca. 1.78-1.76 Ga (Lauri et al., 2022). The point that these reactivated transport pathways facilitated overprinting alterations and mineralization emphasizes the importance of utilizing a tectonic framework for assessing these complex mineral systems.

6. Conclusion

The northern Norrbotten ore province has a complex tectonic evolution and mineralization history and requires that mineral systems assessments be made utilizing a regional tectonic framework. The Pahtohavare-Rakkurijärvi area in the Southern Kiruna mining district hosts syngenetic and epigenetic Cu ± Au and IOCG mineral occurrences which have not been contextualized within the structural evolution of the region. In the Pahtohavare-Rakkurijärvi area, the Rhyacian to lower

https://doi.org/10.5194/egusphere-2022-1475
Preprint. Discussion started: 9 January 2023

Orosirian volcanic, volcaniclastic, and sedimentary bedrock is anticlinally folded and bound by two shear zones trending NW-SE on the southwestern limb, and NE-SW to the east. New structural data show the fold is noncylindrical, has a subvertical to steeply inclined axial plane, with a fold axis plunging to the SE, in agreement with previous work. Bedding sub-parallel foliation shows an accordant folding pattern and structural analysis from thin section shows the foliation is mylonitic and has porphyroclasts with pressure shadows, supporting it is a tectonic fabric. The data constrains the fold in the Pahtohavare-Rakkurijärvi area as F_2 with folded S_1 foliation and axial plane parallel S_2 foliation developed. Importantly, quartz-carbonate-sulfide vein generations related to the epigenetic Cu ± Au Pahtohavare deposits are observed cutting foliation and trending axial plane parallel and at an angle to the F_2 Pahtohavare fold axis trace, structurally constraining the deposits to the late orogenic phase of the Svecokarelian orogeny. These results mark the first time a deposit in the Kiruna mining district has been linked to the late phase of the orogeny. The shear zones binding the fold in the Pahtohavare-Rakkurijärvi area are interpreted to be reactivated early structures and oblique reverse kinematics are proposed for the NW-SE shear zone to explain the geometry of the fold in response to E-W crustal shortening. A time gap of ~80 Myr between the formation of the Kiirunavaara IOA deposit and the formation of the Pahtohavare epigenetic Cu ± Au deposits holds important implications about the timing of iron oxide (apatite) and copper-gold precipitation in Kiruna, showing at least two distinct mineralizing periods can be constrained to different phases of the tectonic evolution.

Author Contributions

L.L. conducted the geological mapping, processed the structural data, sampled, and conducted thin section petrography, visualized the results, wrote the original manuscript, and reviewed and edited the final manuscript. E.Cs.V. made the 3D geologic model from drill logs, visualized the results, wrote sections of the original manuscript, and edited the final manuscript. J.B.H.A. assisted with field work and structural interpretations and edited the final manuscript. O.M. assisted with structural interpretations and edited the final manuscript. T.E.B. secured funding, supervised, assisted with field work and structural interpretations, visualized the results, and edited the final manuscript.

Competing Interests

The authors declare that they have no conflict of interest.

Acknowledgments

This work is part of the European Union's Horizon 2020 project "New Exploration Technologies – NEXT" (Grant Agreement No. 776804). Lovisagruvan AB and Critical Metals Scandinavia AB are thanked for providing access to open pits. Petroleum

https://doi.org/10.5194/egusphere-2022-1475
Preprint. Discussion started: 9 January 2023

Experts Ltd. is thanked for donating the MOVE 2017 software. The staff at the Geological Survey of Sweden is thanked for their help and collaboration during sampling at the National Drill Core Archive in Malå, Sweden.

References

Andersson, J. B. H., Bauer, T. E., and Lynch, E. P.: Evolution of structures and hydrothermal alteration in a Palaeoproterozoic supracrustal belt: Constraining paired deformation–fluid flow events in an Fe and Cu–Au prospective terrain in northern Sweden, Solid Earth, 11, 547–578, https://doi.org/10.5194/se-11-547-2020, 2020.

Andersson, J. B. H., Bauer, T. E., and Martinsson, O.: Structural Evolution of the Central Kiruna Area, Northern Norrbotten, Sweden: Implications on the Geologic Setting Generating Iron Oxide-Apatite and Epigenetic Iron and Copper Sulfides, Econ Geol, 116, 1981–2009, https://doi.org/10.5382/econgeo.4844, 2021.

Andersson, J. B. H., Logan, L., Martinsson, O., Chew, D., Kooijman, E., Kielman-Schmitt, M., Kampmann, T. C., and Bauer, T. E.: U-Pb zircon-titanite-apatite age constraints on basin development and basin inversion in the Kiruna mining district, Sweden, Precambrian Research, 372, 106613, https://doi.org/10.1016/j.precamres.2022.106613, 2022.

BABEL Working Group: Evidence for early Proterozoic plate tectonics from seismic reflection profiles in the Baltic shield, Nature, 348, 34–38, https://doi.org/10.1038/348034a0, 1990.

Barra, F., Reich, M., Selby, D., Rojas, P., Simon, A., Salazar, E., and Palma, G.: Unraveling the origin of the Andean IOCG clan: A Re-Os isotope approach, Ore Geol. Rev., 81, 62–78, https://doi.org/10.1016/j.oregeorev.2016.10.016, 2017.

Barton, M. D.: Iron Oxide(–Cu–Au–REE–P–Ag–U–Co) Systems, in: Treatise on Geochemistry, Elsevier, 515–541, https://doi.org/10.1016/B978-0-08-095975-7.01123-2, 2014.

Bauer, T. E. and Andersson, J. B. H.: Structural controls on Cu-Au mineralization in the Svappavaara area, northern Sweden: The northern continuation of the Nautanen IOCG-system (paper II), in: Paleoproterozoic deformation in the Kiruna-Gällivare area in northern Norrbotten, Sweden: Setting, character, age, and control of iron oxide-apatite deposits (PhD Thesis), edited by: Andersson, J. B. H., Luleå University of Technology, Luleå, Sweden, 1–15, 2021.

Bauer, T. E., Skyttä, P., Allen, R. L., and Weihed, P.: Syn-extensional faulting controlling structural inversion – Insights from the Palaeoproterozoic Vargfors syncline, Skellefte mining district, Sweden, Precambrian Res., 191, 166–183, https://doi.org/10.1016/j.precamres.2011.09.014, 2011.

Bauer, T. E., Andersson, J. B. H., Sarlus, Z., Lund, C., and Kearney, T.: Structural Controls on the Setting, Shape, and Hydrothermal Alteration of the Malmberget Iron Oxide-Apatite Deposit, Northern Sweden, Econ Geol, 113, 377–395, https://doi.org/10.5382/econgeo.2018.4554, 2018.

Bauer, T. E., Lynch, E. P., Sarlus, Z., Drejing-Carroll, D., Martinsson, O., Metzger, N., and Wanhainen, C.: Structural Controls on Iron Oxide Copper-Gold Mineralization and Related Alteration in a Paleoproterozoic Supracrustal Belt: Insights from the Nautanen Deformation Zone and Surroundings, Northern Sweden, Economic Geology, 117, 327–359, https://doi.org/10.5382/econgeo.4862, 2022.

Bergman, S.: Geology of the Northern Norrbotten ore province, northern Sweden, Geological Survey of Sweden, 2018.

https://doi.org/10.5194/egusphere-2022-1475
Preprint. Discussion started: 9 January 2023

Bergman, S. and Weihed, P.: Chapter 3 Archean (>2.6 Ga) and Paleoproterozoic (2.5–1.8 Ga), pre- and syn-orogenic magmatism, sedimentation and mineralization in the Norrbotten and Överkalix lithotectonic units, Svecokarelian orogen, Geological Society, London, Memoirs, 50, 27–81, https://doi.org/10.1144/M50-2016-29, 2020.

Bergman, S., Kübler, L., and Martinsson, O.: Description of regional geological and geophysical maps of northern Norrbotten County (east of the Caledonian orogen), Sveriges geologiska undersökning, Uppsala, 110 pp., 2001.

Bergman, S., Billström, K., Persson, P.-O., Skiöld, T., and Evins, P.: U-Pb age evidence for repeated Palaeoproterozoic metamorphism and deformation near the Pajala shear zone in the northern Fennoscandian shield, GFF, 128, 7–20, https://doi.org/10.1080/11035890601281007, 2006.

Bingen, B., Solli, A., Viola, G., Torgersen, E., Sandstad, J. S., Whitehouse, M. J., Røhr, T. S., Ganerød, M., and Nasuti, A.: Geochronology of the Palaeoproterozoic Kautokeino Greenstone Belt, Finnmark, Norway: Tectonic implications in a Fennoscandia context, NJG, 95, 365–396, https://doi.org/10.17850/njg95-3-09, 2015.

Blomgren, H.: U-Pb Dating of Monazites from the Kiirunavaara and Rektorn Ore Deposits, Master of Science, University of Gothenburg, Gothenburg, 41 pp., 2015.

Cliff, R. A. and Rickard, D.: Isotope systematics of the Kiruna magnetite ores, Sweden; Part 2, Evidence for a secondary event 400 m.y. after ore formation, Econ Geol, 87, 1121–1129, https://doi.org/10.2113/gsecongeo.87.4.1121, 1992.

Cliff, R. A., Rickard, D., and Blake, K.: Isotope systematics of the Kiruna magnetite ores, Sweden; Part 1, Age of the ore, Econ Geol, 85, 1770–1776, https://doi.org/10.2113/gsecongeo.85.8.1770, 1990.

Corriveau, L., Montreuil, J.-F., and Potter, E. G.: Alteration Facies Linkages Among Iron Oxide Copper-Gold, Iron Oxide-Apatite, and Affiliated Deposits in the Great Bear Magmatic Zone, Northwest Territories, Canada, Econ Geol, 111, 2045–2072, https://doi.org/10.2113/econgeo.111.8.2045, 2016.

Day, W. C., Slack, J. F., Ayuso, R. A., and Seeger, C. M.: Regional Geologic and Petrologic Framework for Iron Oxide ± Apatite ± Rare Earth Element and Iron Oxide Copper-Gold Deposits of the Mesoproterozoic St. Francois Mountains Terrane, Southeast Missouri, USA, Economic Geology, 111, 1825–1858, https://doi.org/10.2113/econgeo.111.8.1825, 2016.

Druguet, E.: Deciphering the presence of axial-planar veins in tectonites, Geoscience Frontiers, 10, 2101–2115, https://doi.org/10.1016/j.gsf.2019.02.005, 2019.

Frietsch, R.: Petrology of the Kurravaara Area Northeast of Kiruna northern Sweden, Sveriges Geologiska Undersökning, Uppsala, 1979.

Frietsch, R., Tuisku, P., Martinsson, O., and Perdahl, J.-A.: Early Proterozoic Cu-(Au) and Fe ore deposits associated with regional Na-Cl metasomatism in northern Fennoscandia, Ore Geol. Rev., 12, 1–34, https://doi.org/10.1016/S0169-1368(96)00013-3, 1997.

Geijer, P.: Geology of the Kiruna District 2: Igneous rocks and iron ores of Kiirunavaara, Luossavaara and Tuolluvaara, Stockholm, 1910.

Geijer, P.: Recent Developments at Kiruna, Sveriges Geologiska Undersökning, 22 pp., 1919.

Grigull, S., Berggren, R., Jönnberger, J., Jönsson, C., Hellström, S., and Luth, S.: Folding observed in Paleoproterozoic supracrustal rocks in northern Sweden, Geological Survey of Sweden, 2018.

https://doi.org/10.5194/egusphere-2022-1475
Preprint. Discussion started: 9 January 2023

Groves, D. I., Bierlein, F. P., Meinert, L. D., and Hitzman, M. W.: Iron Oxide Copper-Gold (IOCG) Deposits through Earth History: Implications for Origin, Lithospheric Setting, and Distinction from Other Epigenetic Iron Oxide Deposits, Econ Geol, 105, 641–654, https://doi.org/10.2113/gsecongeo.105.3.641, 2010.

Hietanen, A.: Generation of potassium-poor magmas in the northern Sierra Nevada and the Svecofennian of Finland, J Res US Geol Surv, 3, 631–645, 1975.

Högdahl, K., Andersson, U. B., and Eklund, O. (Eds.): The Transscandinavian Igneous Belt (TIB) in Sweden: a review of its character and evolution, Geological Survey of Finland, Espoo, 125 pp., 2004.

Lahtinen, R., Korja, A., and Nironen, M.: Paleoproterozoic tectonic evolution, in: Precambrian Geology of Finland - Key to the Evolution of the Fennoscandian Shield, edited by: Lehtinen, M., Nurmi, P. A., and Rämö, O. T., Elsevier B.V., Amsterdam, 481–532, 2005.

Lauri, L. S., Miles, J., Liu, X., and O'Brien, H.: Age and C-O isotopes of the hydrothermal breccias within the Kiruna-Naimakka zone, Norrbotten, Sweden, Geological Society of Sweden, 150 year anniversary meeting, Uppsala, 244–245, 2022.

Lindblom, S., Broman, C., and Martinsson, O.: Magmatic-hydrothermal fluids in the Pahtohavare Cu-Au deposit in greenstone at Kiruna, Sweden, 31, 307–318, 1996.

Logan, L., Andersson, J. B. H., Whitehouse, M. J., Martinsson, O., and Bauer, T. E.: Energy Drive for the Kiruna Mining District Mineral System(s): Insights from U-Pb Zircon Geochronology, Minerals, 12, 875, https://doi.org/10.3390/min12070875, 2022.

Lundbohm, H. J.: Sketch of the Geology of the Kiruna district, Geologiska Föreningen i Stockholm Förhandlingar, 32, 751–788, https://doi.org/10.1080/11035891009443831, 1910.

Luth, S., Jönsson, C., Grigull, S., Berggren, R., van Assema, B., Smoor, W., and Djuly, T.: The Pajala deformation belt in northeast Sweden: Structural geological mapping and 3D modelling around Pajala, Geological Survey of Sweden, 2018a.

Luth, S., Jönnberger, J., and Grigull, S.: The Vakko and Kovo greenstone belts: Integrating structural geological mapping and geophysical modelling, Geological Survey of Sweden, 2018b.

Lynch, E. P., Jönberger, J., Bauer, T. E., Sarlus, Z., and Martinsson, O.: Barents project 2014: Meta-volcanosedimentary rocks in the Nautanen area, Norrbotten: preliminary lithological and deformation characteristics, Sveriges geologiska undersökning, Uppsala, 2015.

Martinsson, O.: Tectonic Setting and Metallogeny of the Kiruna Greenstones, Doctoral Thesis, Luleå tekniska universitet, Lulea, Sweden, 162 pp., 1997.

Martinsson, O.: Geology and Metallogeny of the Northern Norrbotten Fe-Cu-Au Province, in: Svecofennian ore-forming environments of northern Sweden- volcanic associated Zn-Cu-Au-Ag, intrusion related Cu-Au, sediment hosted Pb-Zn, and magnetite-apatite deposits in northern Sweden, edited by: Allen, R. L., Martinsson, O., and Weihed, P., Society of Economic Geologists, 131–148, 2004.

Martinsson, O.: Genesis of the Per Geijer apatite iron ores, Kiruna area, northern Sweden, SGA biennial meeting 2015, Nancy, France, 23–27, 2015.

https://doi.org/10.5194/egusphere-2022-1475
Preprint. Discussion started: 9 January 2023

Martinsson, O. and Hansson, K.-E.: Apatite Iron Ores in the Kiruna Area, in: Svecofennian ore-forming environments of northern Sweden- volcanic associated Zn-Cu-Au-Ag, intrusion related Cu-Au, sediment hosted Pb-Zn, and magnetite-apatite deposits in northern Sweden, vol. 33, Society of Economic Geologists, 173–175, 2004.

Martinsson, O. and Perdahl, J.-A.: Paleoproterozoic extensional and compressional magmatism in northern Norrbotten, northern Sweden (Paper II), in: Svecofennian volcanism in northernmost Sweden (PhD Thesis), edited by: Perdahl, J.-A., Luleå University of Technology, Luleå, Sweden, 161, 1995.

Martinsson, O., Perdahl, J.-A., and Bergman, J.: Greenstone and porphyry hosted ore deposits in northern Norrbotten, Nutek, 1993.

Martinsson, O., Hallberg, A., Söderholm, K., and Billström, K.: Pahtohavare - an epigenetic Cu-Au deposit in the Paleoproterzoic Kiruna Greenstones (Paper III), in: Tectonic Setting and Metallogeny of the Kiruna Greenstones (PhD Thesis), edited by: Martinsson, O., Luleå University of Technology, Luleå, Sweden, 37, 1997a.

Martinsson, O., Hallberg, A., Broman, C., Godin-Jonasson, L., Kisiel, T., and Fallick, A. E.: Viscaria - a syngenetic exhalative Cu-deposit in the Paleoproterozoic Kiruna Greenstones (Paper II), in: Tectonic Setting and Metallogeny of the Kiruna Greenstones (PhD Thesis), edited by: Martinsson, O., Luleå University of Technology, Luleå, Sweden, 57, 1997b.

Martinsson, O., Vaasjoki, M., and Persson, P.-O.: U-Pb zircon ages of Archaean to Palaeoproterozoic granitoids in the Torneträsk–Råstojaure area, northern Sweden, in: Radiometric dating results 4, Geological Survey of Sweden, Uppsala, 70–90, 1999.

Martinsson, O., Billström, K., Broman, C., Weihed, P., and Wanhainen, C.: Metallogeny of the Northern Norrbotten Ore Province, northern Fennoscandian Shield with emphasis on IOCG and apatite-iron ore deposits, Ore Geol. Rev., 78, 447–492, https://doi.org/10.1016/j.oregeorev.2016.02.011, 2016.

Martinsson, O., Bergman, S., Persson, P.-O., Schöberg, H., Billström, K., and Shumlyanksyy, L.: Stratigraphy and ages of Palaeoproterozoic metavolcanic and metasedimentary rocks at Käymäjärvi, northern Sweden, Geological Survey of Sweden, 2018.

Mellqvist, C.: The Archaean–Proterozoic Palaeoboundary in the Luleå area, northern Sweden: field and isotope geochemical evidence for a sharp terrane boundary, Precambrian Research, 96, 225–243, https://doi.org/10.1016/S0301-9268(99)00011-X, 1999.

Naslund, H. R., Henríquez, F., Nyström, J. O., Vivallo, W., and Dobbs, F. M.: Magmatic iron ores and associated mineralisation: Examples from the Chilean High Andes and Coastal Cordillera, in: Hydrothermal Iron Oxide-Copper-Gold & Related Deposits: A Global Perspective, vol. 2, PCG Publishing, Adelaide, 207–226, 2002.

Nyström, J. O. and Henriquez, F.: Magmatic features of iron ores of the Kiruna type in Chile and Sweden; ore textures and magnetite geochemistry, Economic Geology, 89, 820–839, https://doi.org/10.2113/gsecongeo.89.4.820, 1994.

Öhlander, B., Skiöld, T., Elming, S.-Å., Claesson, S., and Nisca, D. H.: Delineation and character of the Archaean-Proterozoic boundary in northern Sweden, Precambrian Res., 64, 67–84, https://doi.org/10.1016/0301-9268(93)90069-E, 1993.

Parák, T.: The origin of the Kiruna iron ores, C. Davidsons Boktryckeri AB, Stockholm, 209 pp., 1975.

Perdahl, J.-A. and Frietsch, R.: Petrochemical and petrological characteristics of 1.9 Ga old volcanics in northern Sweden, Precambrian Res., 64, 239–252, https://doi.org/10.1016/0301-9268(93)90079-H, 1993.

https://doi.org/10.5194/egusphere-2022-1475
Preprint. Discussion started: 9 January 2023

Pharaoh, T. C. and Pearce, J. A.: Geochemical evidence for the geotectonic setting of early Proterozoic metavolcanic sequences in Lapland, Precambrian Res., 25, 283–308, https://doi.org/10.1016/0301-9268(84)90037-8, 1984.

del Real, I., Reich, M., Simon, A. C., Deditius, A., Barra, F., Rodríguez-Mustafa, M. A., Thompson, J. F. H., and Roberts, M. P.: Formation of giant iron oxide-copper-gold deposits by superimposed, episodic hydrothermal pulses, Commun Earth Environ, 2, 192, https://doi.org/10.1038/s43247-021-00265-w, 2021.

Reich, M., Simon, A. C., Deditius, A., Barra, F., Chryssoulis, S., Lagas, G., Tardani, D., Knipping, J., Bilenker, L., Sanchez-Alfaro, P., Roberts, M. P., and Munizaga, R.: Trace element signature of pyrite from the Los Colorados iron oxide-apatite (IOA) deposit, Chile; a missing link between Andean IOA and iron oxide copper-gold systems?, Economic Geology and the Bulletin of the Society of Economic Geologists, 111, 743–761, https://doi.org/10.2113/econgeo.111.3.743, 2016.

Reich, M., Simon, A. C., Barra, F., Palma, G., Hou, T., and Bilenker, L. D.: Formation of iron oxide–apatite deposits, Nat Rev Earth Environ, 3, 758–775, https://doi.org/10.1038/s43017-022-00335-3, 2022.

Romer, R. L.: U-Pb systematics of stilbite-bearing low-temperature mineral assemblages from the Malmberget iron ore, northern Sweden, Geochemica et Cosmochimica Acta, 60, 1951–1961, 1996.

Romer, R. L., Martinsson, O., and Perdahl, J. A.: Geochronology of the Kiruna iron ores and hydrothermal alterations, Economic Geology, 89, 1249–1261, https://doi.org/10.2113/gsecongeo.89.6.1249, 1994.

Sarlus, Z., Andersson, U. B., Bauer, T. E., Wanhainen, C., Martinsson, O., Nordin, R., and Andersson, J. B. H.: Timing of plutonism in the Gällivare area: implications for Proterozoic crustal development in the northern Norrbotten ore district, Sweden, Geol. Mag., 155, 1351–1376, https://doi.org/10.1017/S0016756817000280, 2018.

Sarlus, Z., Andersson, U. B., Martinsson, O., Bauer, T. E., Wanhainen, C., Andersson, J. B. H., and Whitehouse, M. J.: Timing and origin of the host rocks to the Malmberget iron oxide-apatite deposit, Sweden, Precambrian Res., 342, 105652, https://doi.org/10.1016/j.precamres.2020.105652, 2020.

Sillitoe, R. H.: Iron oxide-copper-gold deposits: an Andean view, Mineralium Deposita, 38, 787–812, https://doi.org/10.1007/s00126-003-0379-7, 2003.

Simon, A. C., Knipping, J., Reich, M., Barra, F., Deditius, A. P., Bilenker, L., and Childress, T.: Kiruna-Type Iron Oxide-Apatite (IOA) and Iron Oxide Copper-Gold (IOCG) Deposits Form by a Combination of Igneous and Magmatic-Hydrothermal Processes: Evidence from the Chilean Iron Belt, in: Metals, Minerals, and Society, Society of Economic Geologists (SEG), https://doi.org/10.5382/SP.21.06, 2018.

Skiöld, T.: Implications of new U-Pb zircon chronology to early Proterozoic crustal accretion in northern Sweden, Precambrian Res., 38, 147–164, https://doi.org/10.1016/0301-9268(88)90089-7, 1988.

Skirrow, R. G.: Iron oxide copper-gold (IOCG) deposits – a review (part 1): settings, mineralogy, ore geochemistry, and classification, Ore Geol. Rev., 104569, https://doi.org/10.1016/j.oregeorev.2021.104569, 2021.

Skyttä, P., Bauer, T. E., Tavakoli, S., Hermansson, T., Andersson, J., and Weihed, P.: Pre-1.87Ga development of crustal domains overprinted by 1.87Ga transpression in the Palaeoproterozoic Skellefte district, Sweden, Precambrian Res., 206–207, 109–136, https://doi.org/10.1016/j.precamres.2012.02.022, 2012.

Skyttä, P., Määttä, M., Palsatech Oy, Piippo, S., Kara, J., Käpyaho, A., Heilimo, E., and O'Brien, H.: Constraints over the age of magmatism and subsequent deformation for the Neoarchean Kukkola Gneiss Complex, northern Fennoscandia, Bull Geol Soc Finland, 92, 19–38, https://doi.org/10.17741/bgsf/92.1.002, 2020.

https://doi.org/10.5194/egusphere-2022-1475
Preprint. Discussion started: 9 January 2023

Smith, M., Coppard, J., Herrington, R., and Stein, H.: The Geology of the Rakkurijärvi Cu-(Au) Prospect, Norrbotten: A New Iron Oxide-Copper-Gold Deposit in Northern Sweden, Economic Geology, 102, 393–414, https://doi.org/10.2113/gsecongeo.102.3.393, 2007.

Smith, M., Coppard, J., and Herrington, R.: The geology of the Rakkurijärvi copper-prospect, Norrbotten county, Sweden, in: Hydrothermal Iron Oxide Copper-Gold and Related Deposits: A Global Perspective, vol. v.4-Advances in the Understanding of IOCG Deposits, edited by: Porter, T. M., PGC Publishing, Adelaide, 427–440, 2010.

Smith, M. P., Storey, C. D., Jeffries, T. E., and Ryan, C.: In Situ U-Pb and Trace Element Analysis of Accessory Minerals in the Kiruna District, Norrbotten, Sweden: New Constraints on the Timing and Origin of Mineralization, Journal of Petrology, 50, 2063–2094, https://doi.org/10.1093/petrology/egp069, 2009.

Storey, C. D., Smith, M. P., and Jeffries, T. E.: In situ LA-ICP-MS U–Pb dating of metavolcanics of Norrbotten, Sweden: Records of extended geological histories in complex titanite grains, Chemical Geology, 240, 163–181, https://doi.org/10.1016/j.chemgeo.2007.02.004, 2007.

Tornos, F.: Magnetite-Apatite and IOCG deposits formed by magmatic-hydrothermal evolution of complex calc-alkaline melts, in: Eleventh Biennial SGA Meeting, Let's talk ore deposits, Antofagasta, Chile, 26–28, 2011.

Tornos, F., Velasco, F., and Hanchar, J. M.: The Magmatic to Magmatic-Hydrothermal Evolution of the El Laco Deposit (Chile) and Its Implications for the Genesis of Magnetite-Apatite Deposits, Economic Geology, 112, 1595–1628, https://doi.org/10.5382/econgeo.2017.4523, 2017.

Troll, V. R., Weis, F. A., Jonsson, E., Andersson, U. B., Majidi, S. A., Högdahl, K., Harris, C., Millet, M.-A., Chinnasamy, S. S., Kooijman, E., and Nilsson, K. P.: Global Fe–O isotope correlation reveals magmatic origin of Kiruna-type apatite-iron-oxide ores, Nat Commun, 10, 1712, https://doi.org/10.1038/s41467-019-09244-4, 2019.

Velasco, F., Tornos, F., and Hanchar, J. M.: Immiscible iron- and silica-rich melts and magnetite geochemistry at the El Laco volcano (northern Chile): Evidence for a magmatic origin for the magnetite deposits, Ore Geol. Rev., 79, 346–366, https://doi.org/10.1016/j.oregeorev.2016.06.007, 2016.

Vollmer, F. W., Wright, S. F., and Hudleston, P. J.: Early deformation in the Svecokarelian greenstone belt of the Kiruna iron district, northern Sweden, Geologiska Föreningen i Stockholm Förhandlingar, 106, 109–118, https://doi.org/10.1080/11035898409454620, 1984.

Wanhainen, C., Billström, K., Martinsson, O., Stein, H., and Nordin, R.: 160 Ma of magmatic/hydrothermal and metamorphic activity in the Gällivare area: Re–Os dating of molybdenite and U–Pb dating of titanite from the Aitik Cu–Au–Ag deposit, northern Sweden, Miner Deposita, 40, 435–447, https://doi.org/10.1007/s00126-005-0006-x, 2005.

Wanhainen, C., Broman, C., Martinsson, O., and Magnor, B.: Modification of a Palaeoproterozoic porphyry-like system: Integration of structural, geochemical, petrographic, and fluid inclusion data from the Aitik Cu–Au–Ag deposit, northern Sweden, Ore Geol. Rev., 48, 306–331, https://doi.org/10.1016/j.oregeorev.2012.05.002, 2012.

Weihed, P. and Williams, P. J.: Metallogeny of the northern Fennoscandian Shield: a set of papers on Cu–Au and VMS deposits of northern Sweden, Miner Deposita, 40, 347–350, https://doi.org/10.1007/s00126-005-0022-x, 2005.

Weihed, P., Billström, K., Persson, P.-O., and Weihed, J. B.: Relationship between 1.90–1.85 Ga accretionary processes and 1.82–1.80 Ga oblique subduction at the Karelian craton margin, Fennoscandian Shield, GFF, 124, 163–180, https://doi.org/10.1080/11035890201243163, 2002.

https://doi.org/10.5194/egusphere-2022-1475
Preprint. Discussion started: 9 January 2023

Welin, E.: The depositional evolution of the Svecofennian supracrustal sequence in Finland and Sweden, Precambrian Res., 35, 95–113, https://doi.org/10.1016/0301-9268(87)90047-7, 1987.

Westhues, A., Hanchar, J. M., Whitehouse, M. J., and Martinsson, O.: New Constraints on the Timing of Host-Rock Emplacement, Hydrothermal Alteration, and Iron Oxide-Apatite Mineralization in the Kiruna District, Norrbotten, Sweden, Economic Geology, 111, 1595–1618, https://doi.org/10.2113/econgeo.111.7.1595, 2016.

Westhues, A., Hanchar, J. M., Voisey, C. R., Whitehouse, M. J., Rossman, G. R., and Wirth, R.: Tracing the fluid evolution of the Kiruna iron oxide apatite deposits using zircon, monazite, and whole rock trace elements and isotopic studies, Chemical Geology, 466, 303–322, https://doi.org/10.1016/j.chemgeo.2017.06.020, 2017.

Williams, P. J., Barton, M. D., Johnson, D. A., Fontboté, L., Haller, A. de, Mark, G., Oliver, N. H. S., and Marschik, R.: Iron Oxide Copper-Gold Deposits - Geology, Space-Time Distribution, and Possible Modes of Origin, in: One Hundredth Anniversary Volume, Society of Economic Geologists, Littleton, USA, 371–405, https://doi.org/10.5382/AV100.13, 2005.

Witschard, F.: The geological and tectonic evolution of the Precambrian of northern Sweden - A case for basement reactivation?, Precambrian Res., 23, 273–315, https://doi.org/10.1016/0301-9268(84)90047-0, 1984.

Wright, S.: Early Proterozoic Deformational History of the Kiruna District, Northern Sweden, Doctoral Thesis, University of Minnesota, 170 pp., 1988.

Wyborn, L. A. I., Heinrich, C. A., and Jaques, A. L.: Australian Proterozoic Mineral Systems: Essential Ingredients and Mappable Criteria, in: Australasian Institute of Mining and Metallurgy Publication Series, the AusIMM Annual Conference, Darwin, Australia, 109–115, 1994.

https://doi.org/10.5194/egusphere-2022-1475
Preprint. Discussion started: 9 January 2023

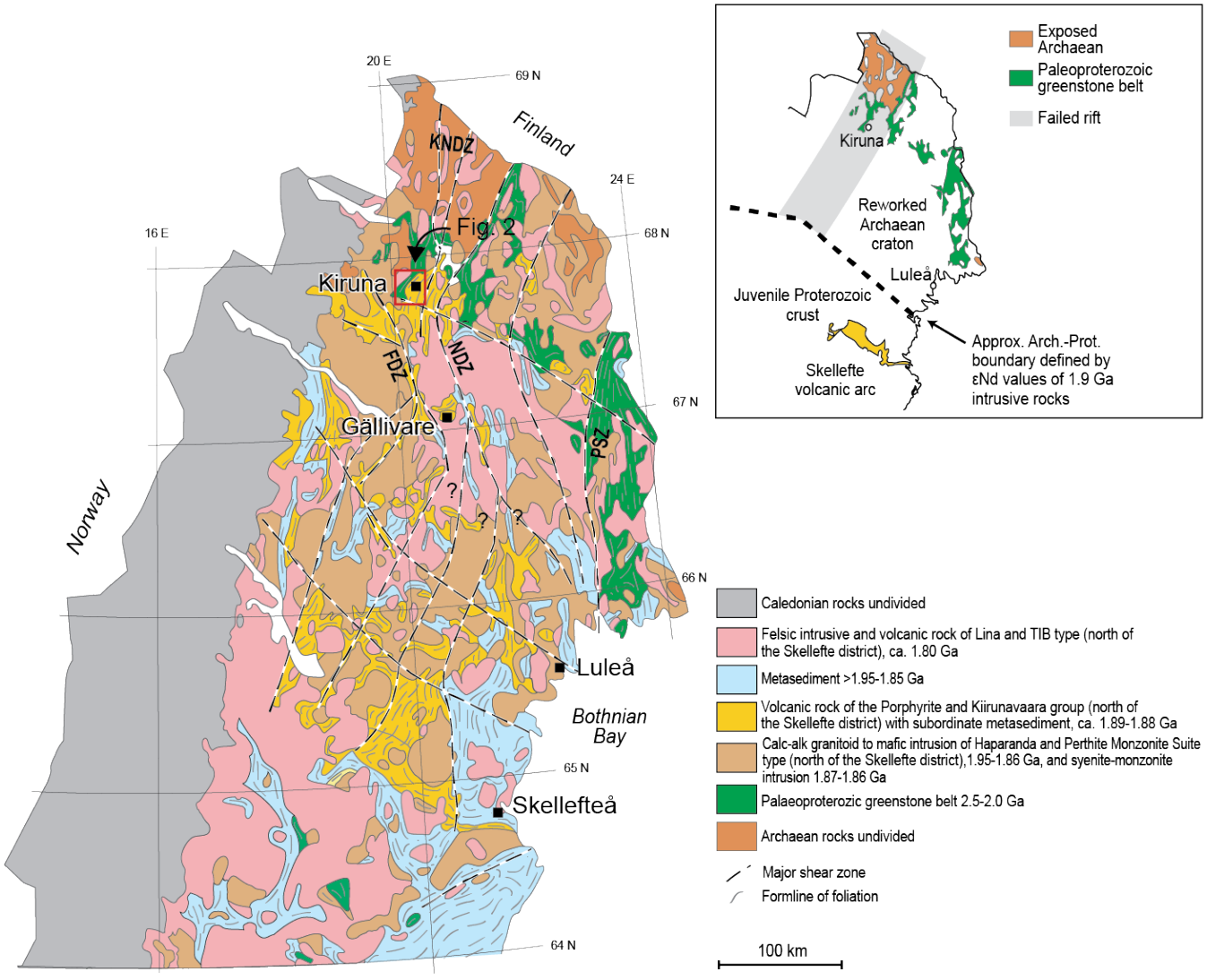

Figure 1: Geologic map of northern Sweden with both the Skellefte district and the northern Norrbotten ore province included. Inset shows approximate paleoboundary of the Archean craton defined by εNd values (Öhlander et al., 1993). FDZ = Fjällåsen deformation zone, KNDZ = Kiruna-Naimakka deformation zone, NDZ = Nautanen deformation zone, PSZ = Pajala shear zone. Modified after Bauer et al. (2022), Weihed and Williams (2005), and Bauer and Andersson (2021).

https://doi.org/10.5194/egusphere-2022-1475
Preprint. Discussion started: 9 January 2023

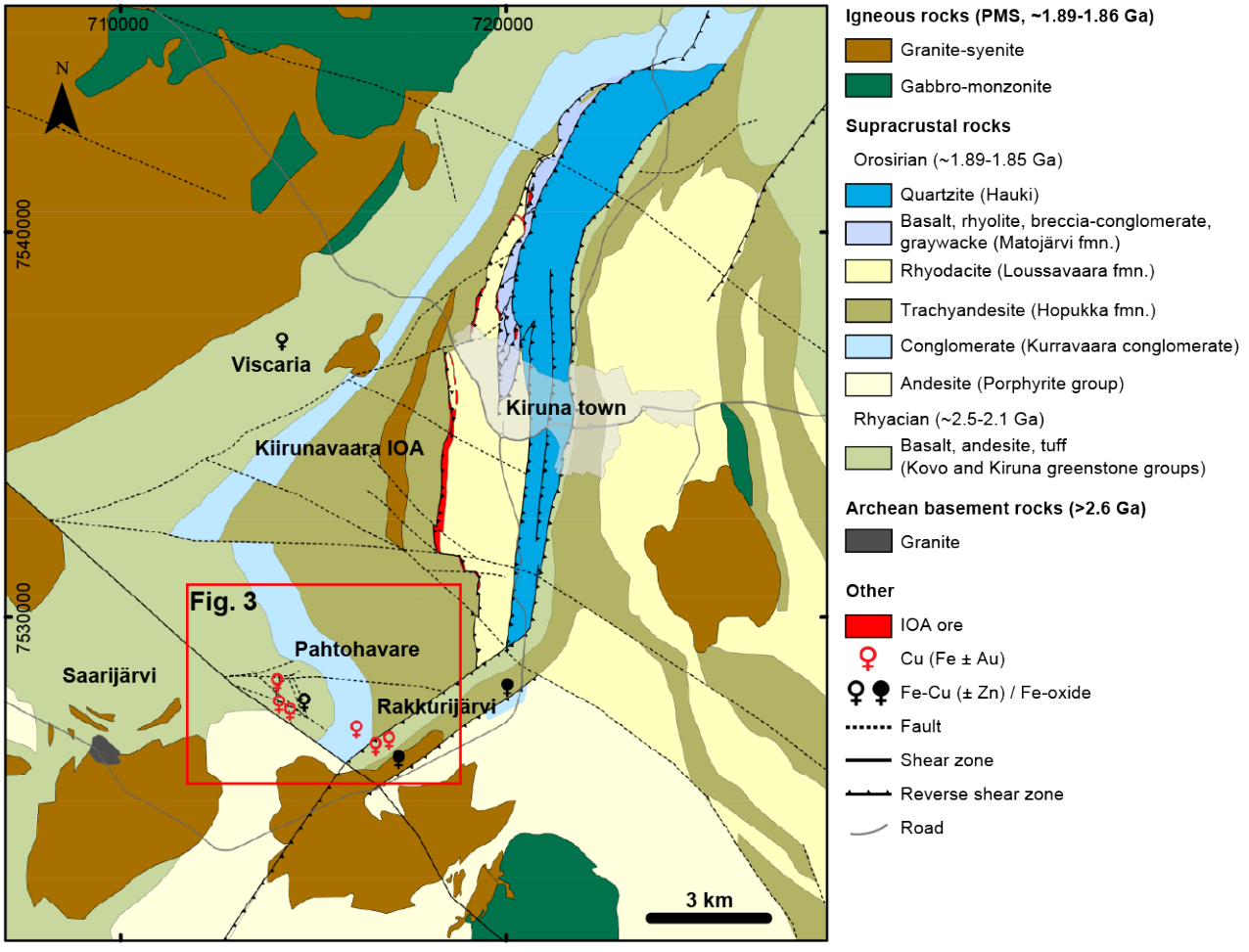

Figure 2: Geologic map of the Kiruna mining district showing stratigraphy, structures, and igneous intrusions. Kiruna town is marked in transparent gray. Cu (Fe ± Au), Fe-Cu (± Zn), and Fe-oxide occurrences are shown as well as local area names. Modified after Martinsson et al. (1993) and Andersson et al. (2021). Coordinate system in SWEREF99.

https://doi.org/10.5194/egusphere-2022-1475
Preprint. Discussion started: 9 January 2023

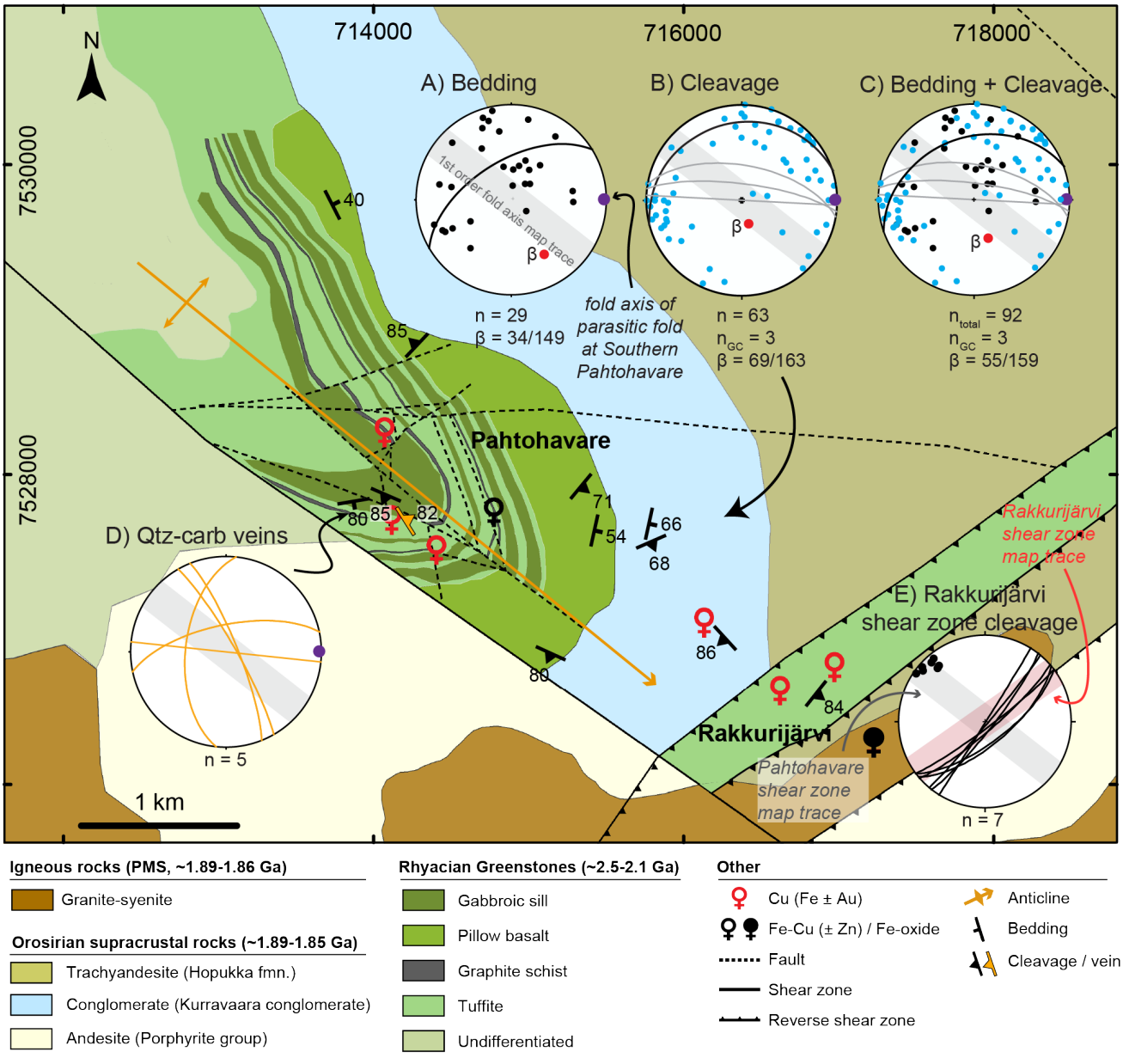

Figure 3: Geologic map of the Pahtohavare and Rakkurijärvi areas with structural results. Lower hemisphere, equal area stereographic projections of structures in the Pahtohavare and Rakkurijärvi area showing A) bedding, B) cleavage, C) combined bedding and cleavage, D) quartz-carbonate vein orientations at Southern Pahtohavare open pit, E) cleavage measurements near the Rakkurijärvi shear zone. Gray band shows the apparent fold axis map trace. Gray great circles (GC) indicate axial subparallel veins to the parasitic fold (fold axis = purple dot) at Pahtohavare southern open pit. Modified after Martinsson et al. (1993) and Martinsson (1997). Coordinate system in SWEREF99.

https://doi.org/10.5194/egusphere-2022-1475
Preprint. Discussion started: 9 January 2023

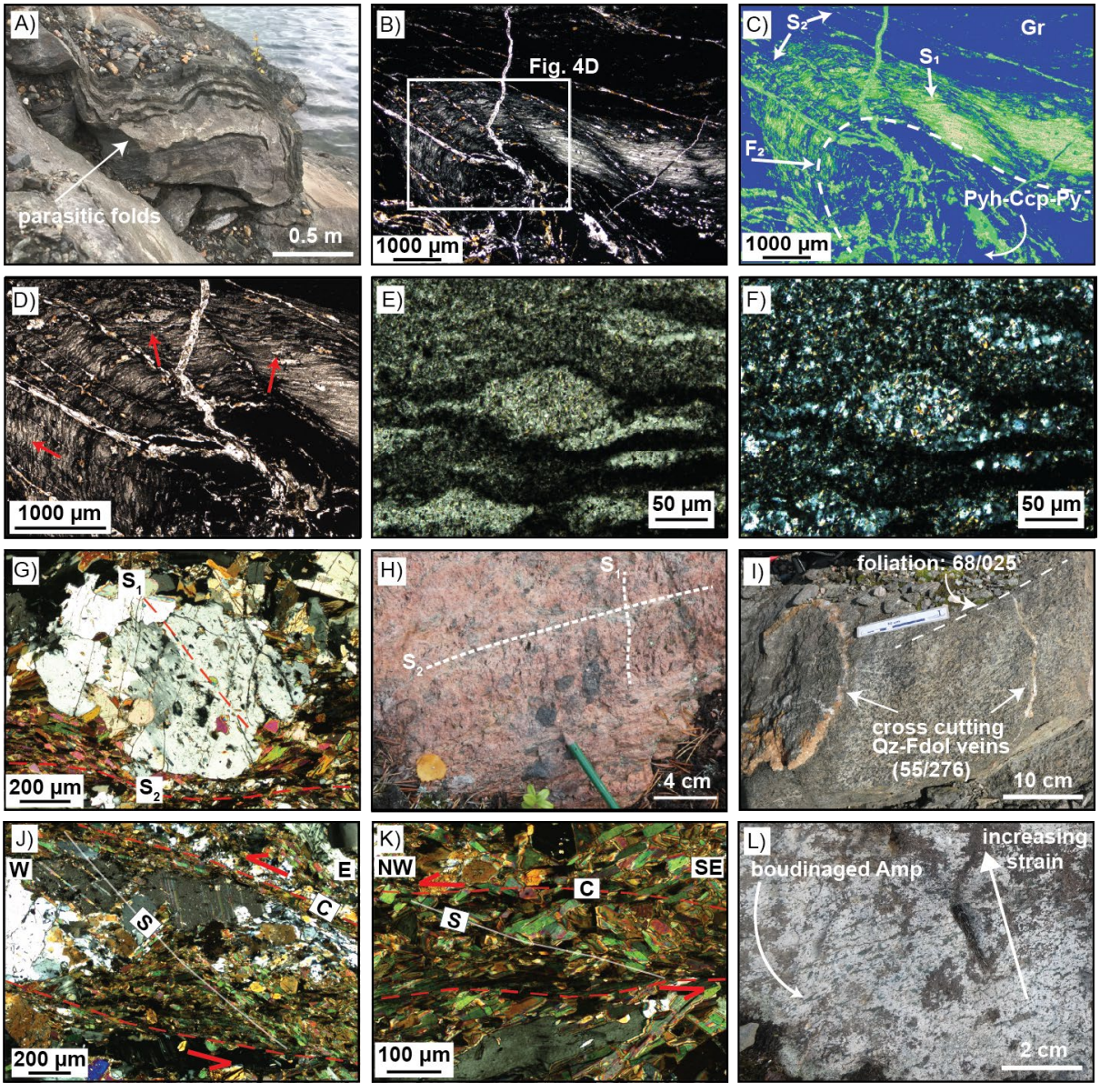

Figure 4: Photographs of structural features in the Pahtohavare-Rakkurijärvi areas. A) Parasitic folds in tuffitic layers as a part of a bigger fold system. Photo taken at Pahtohavare Southern open pit. View southeast, B) Micro-scale fold in graphitic schist from Eastern Pahtohavare. Photo in plane polarized light, C) False color image of graphitic schist in 4B showing S_1, F_2, S_2 and remobilized chalcopyrite, pyrite, and pyrrhotite in the fold hinge and in spaced axial planar cleavage, D) Plane polarized light image of the hinge zone of the graphite schist, showing asymmetric sigmoidal clasts, E) Plane polarized light of an asymmetric sigmoidal clast with recrystallized pressure shadows showing non-coaxial strain, F) Cross polarized light (XPL) of the same clast, G) Scapolite porphyroblast showing preserved foliation trails (S_1) and wrapped by a foliation defined by biotite (S_2), H) Granitic intrusion SW of Pahtohavare showing two directions of tectonic cleavage, I) Foliated mafic sill with Qtz-Fdol veins cross cutting at a high angle at Pahtohavare Southern open pit. View northeast, J)-K) S-C fabric in an oriented sample from a shear band in Pahtohavare Southern open pit showing a sinistral sense of shear. XPL, L) Strain partitioning of amphibole seen in outcrop-scale in Rakkurijärvi. Weakly strained amphibole occurs at the bottom of the outcrop and boudinaged amphibole grains occur towards the top. View towards east. Structural measurements: dip/dip azimuth. Gr = graphite, Pyh = pyrrhotite, Ccp = chalcopyrite, Py = pyrite, Qz = quartz, Fdol = ferrodolomite, Amp = amphibole.

https://doi.org/10.5194/egusphere-2022-1475
Preprint. Discussion started: 9 January 2023

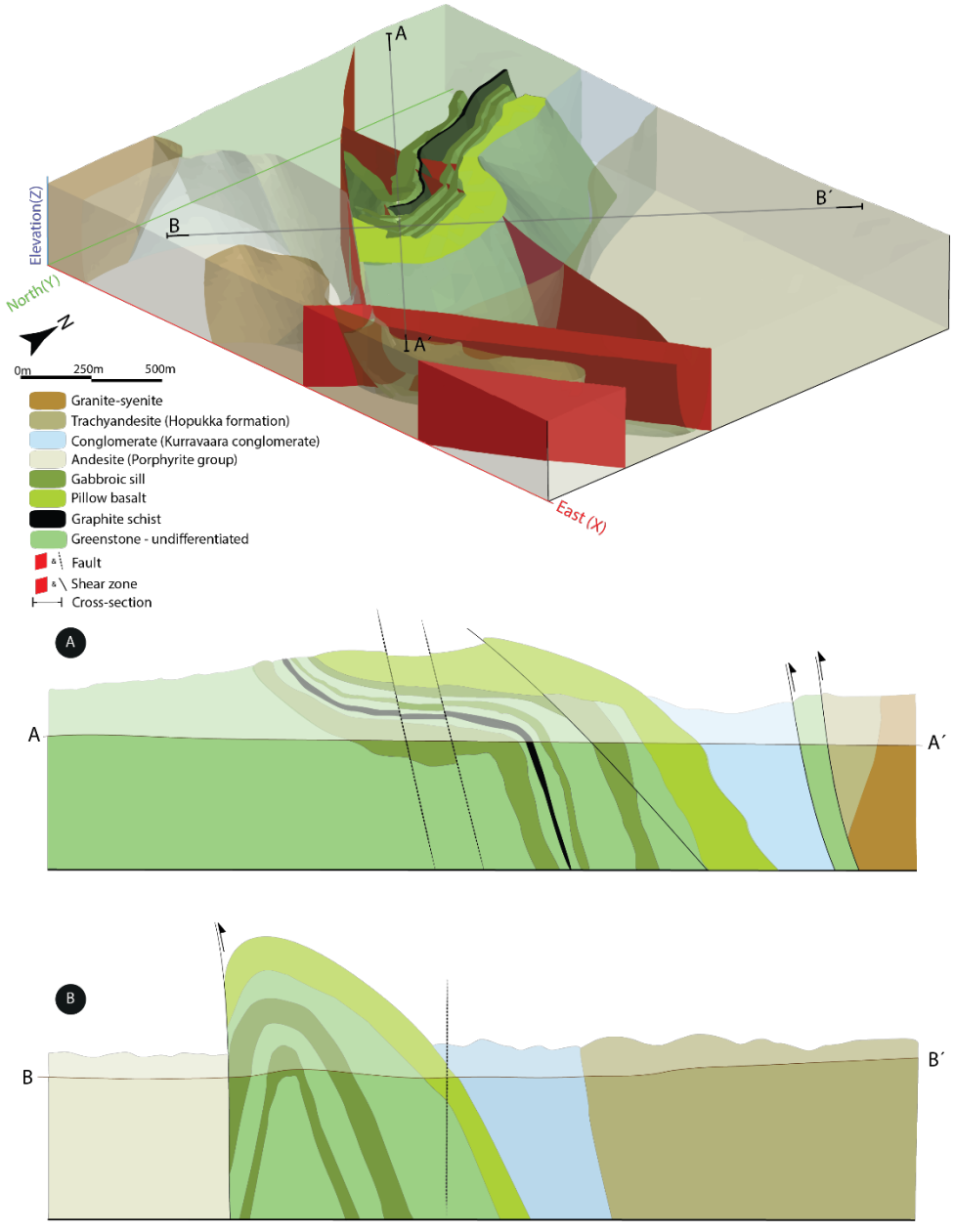

Figure 5: Local 3D model (viewed from above and SE) and conceptual cross-sections of the southern Kiruna mining district, showing the major lithological boundaries, faults and shear-zones. The geological 3D model is built based on the local geological map, structural measurements, and lithological drill hole logs, and highlights the Pahtohavare F_2 fold by utilizing different transparency levels of the adjacent lithological units. The conceptual cross-sections interpreted from the 3D model and structural data in this study highlight the relationship between brittle-ductile structures and local lithostratigraphic units from, A) NW-SE orientation, and B) SW-NE orientation.

https://doi.org/10.5194/egusphere-2022-1475
Preprint. Discussion started: 9 January 2023

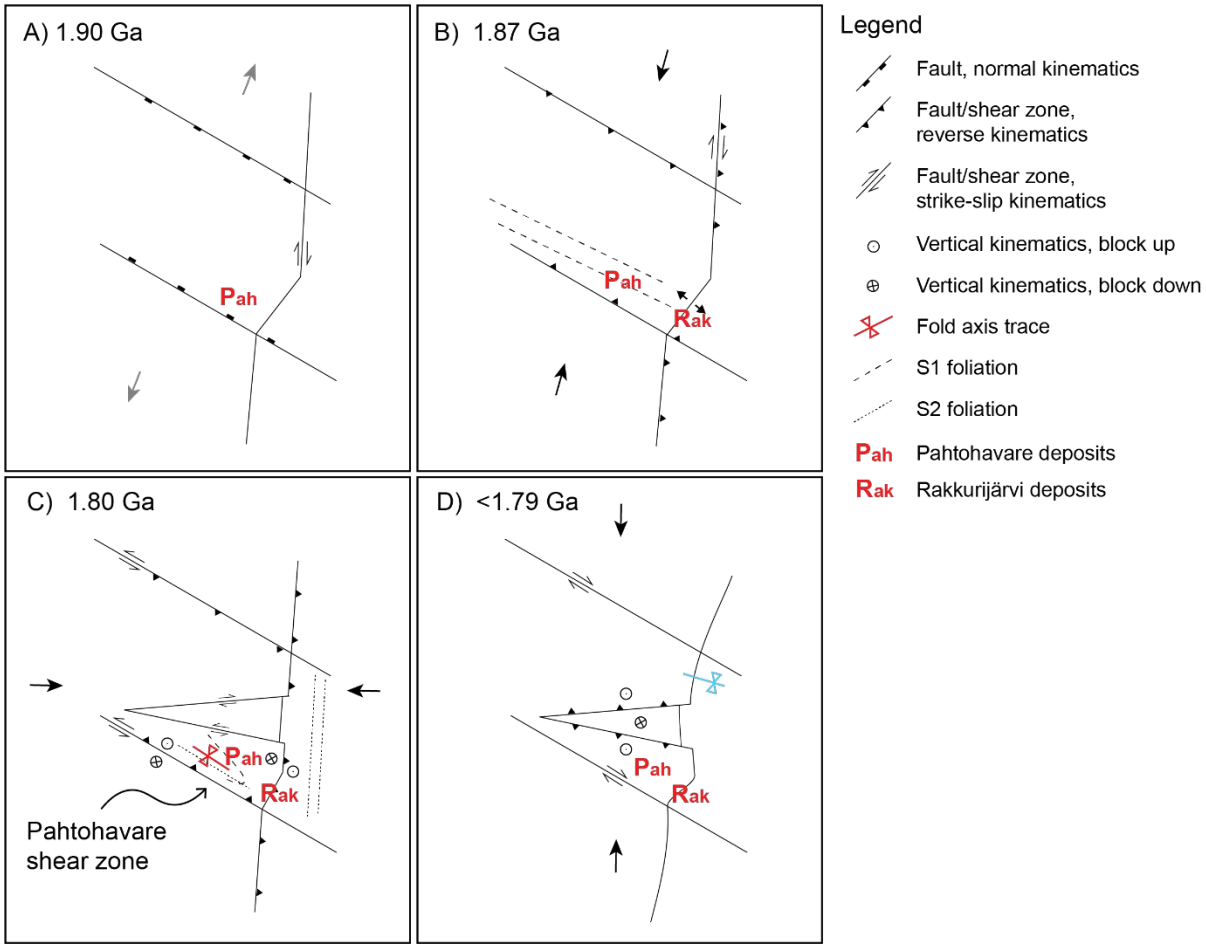

745 **Figure 6: A proposal for the structural framework for the Kiruna mining district. A) The onset of the Svecokarelian orogeny and back arc extension forms and/or reutilizes preexisting normal faults, additional transtensional faults form. The earliest ca. 2.1 Ga Pahtohavare syngenetic deposit (Eastern) has already formed, B) NE-SW crustal shortening from the early Sveocokarelian orogeny reactivates preexisting faults structures, forming transpressional shear zones and dilatational jogs. The Rakkurijärvi IOCG forms (Rak). Early S_1 fabric develops in the southern Kiruna mining district, C) Late orogenic E-W crustal shortening and basin inversion**
750 **occurs. Stratigraphy in the Pahtohavare-Rakkurijärvi area is folded and S_2 foliation develops. Strong strain partitioning occurs with S_2 fabric forming along shear zones in the central Kiruna area. Both brittle and ductile structures form. D) N-S crustal shortening causes gentle refolding in the district and minor reactivation of preexisting structures occurs.**

https://doi.org/10.5194/egusphere-2022-1475
Preprint. Discussion started: 9 January 2023

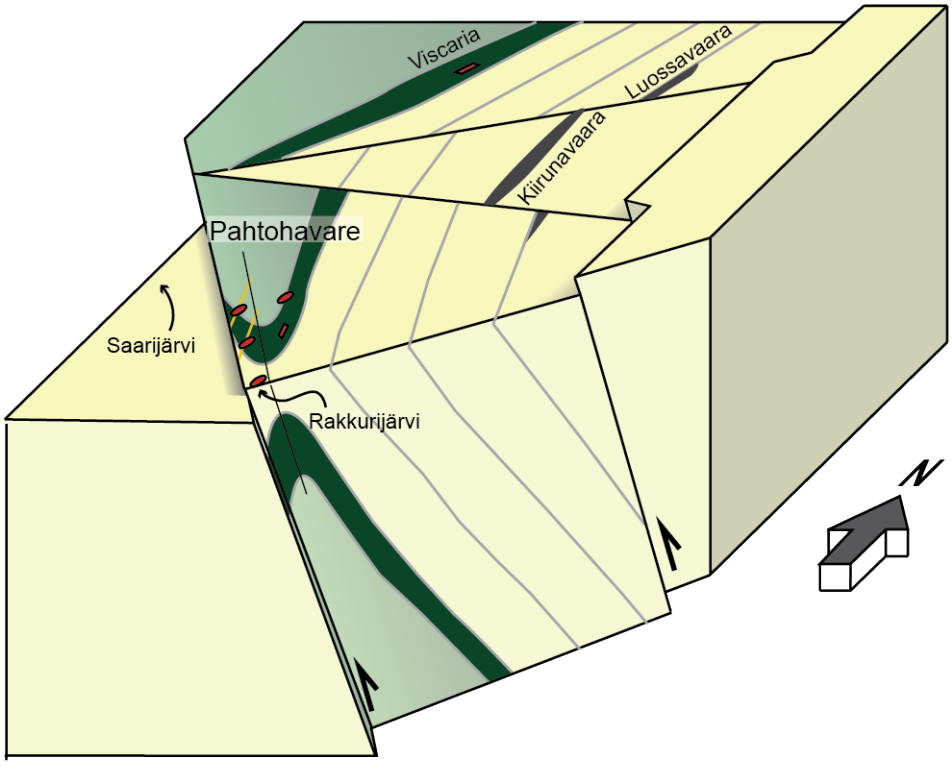

Figure 7: 3D conceptual model of the Pahtohavare area in the southern Kiruna mining district showing the oblique reverse NW-SE trending shear zone and the resultant Pahtohavare F_2 fold. The axial surface is steeply dipping and the Pahtohavare epigenetic deposits are controlled by D_2 structures. Green colors denote older greenstone stratigraphy (ca. >2.1 Ga) and yellow colors denote ca. 1.92 Ga and younger stratigraphy.